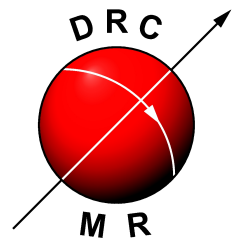


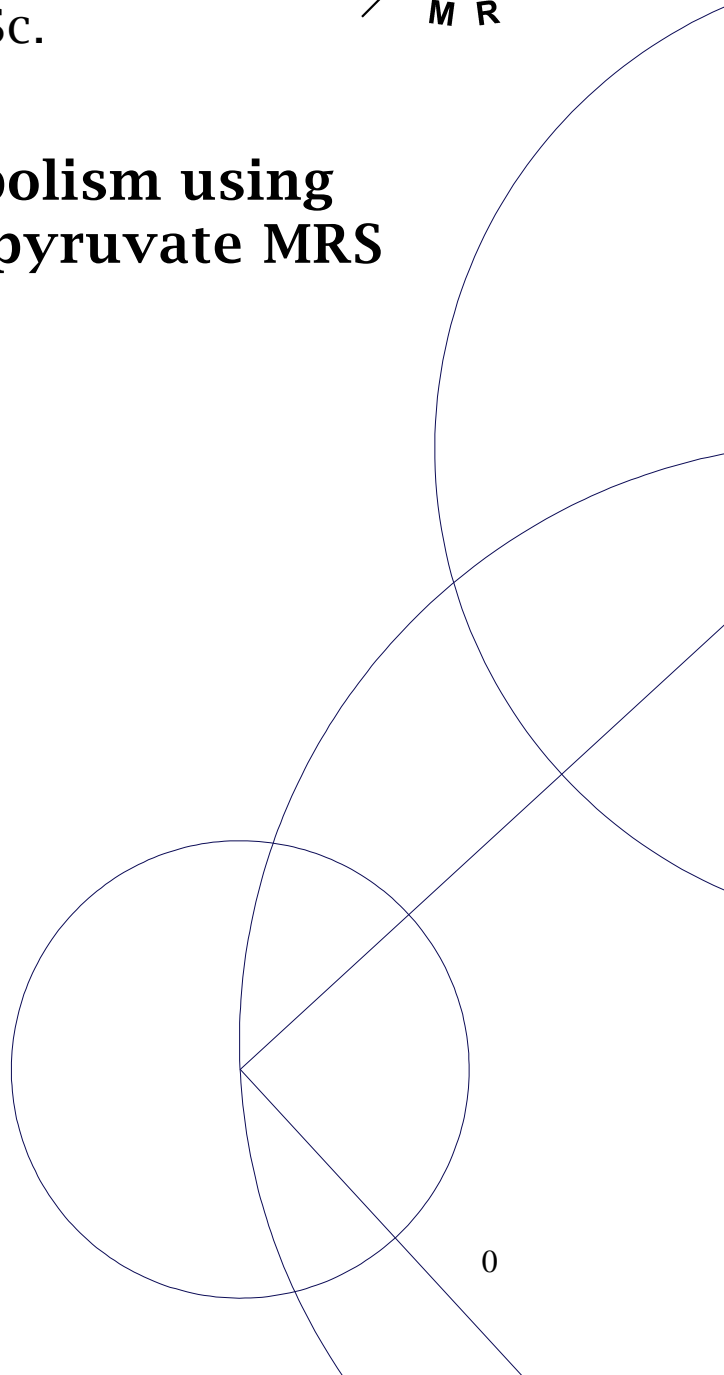
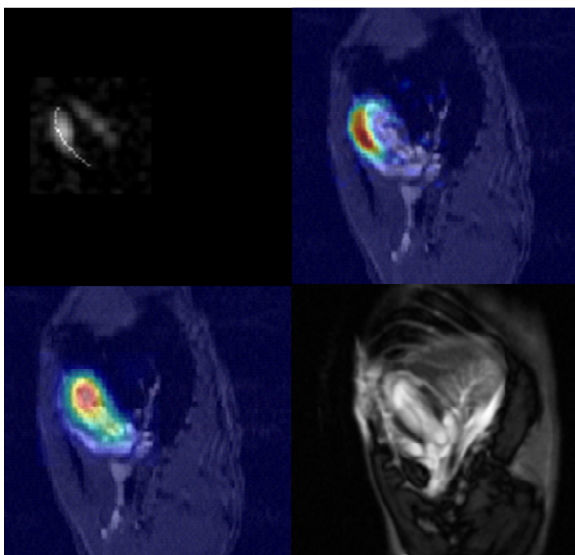


## PhD thesis

Mette Hauge Lauritzen MSc.



# Imaging Cardiac Metabolism using Hyperpolarized $[1-^{13}\text{C}]$ pyruvate MRS





# **Imaging Cardiac Metabolism using Hyperpolarized [1-<sup>13</sup>C]pyruvate MRS**

PhD thesis

Mette Hauge Lauritzen MSc.

Danish Research Centre for Magnetic Resonance, Centre for  
Functional and Diagnostic Imaging and Research, Copenhagen  
University Hospital Hvidovre, Denmark

December 2013

### **Academic Advisor**

Olaf B. Paulson<sup>1,4</sup> (Professor, DMSc)

### **Project supervisors:**

Per Åkeson<sup>1</sup> (DMSc, PhD)

Lise Vejby Søgaard<sup>1</sup>(PhD)

Peter Magnusson<sup>1</sup>(PhD)

Jan Henrik Ardenkjær-Larsen<sup>1,2,3</sup> (PhD)

### **Affiliations**

<sup>1</sup> Danish Research Centre for Magnetic Resonance, Centre for Functional and Diagnostic Imaging and Research, Copenhagen University Hospital Hvidovre, Denmark

<sup>2</sup> GE Healthcare, Brøndby, Denmark

<sup>3</sup> Technical University of Denmark, Department of Electrical Engineering, Kgs. Lyngby, Denmark

<sup>4</sup> Neurobiology Research Unit. Rigshospitalet. Copenhagen University Hospital Denmark.

The thesis is based on studies performed in collaboration between the faculty of Health and Medical Sciences Copenhagen University, Denmark and the Danish Research Centre for Magnetic Resonance, Centre for Functional and Diagnostic Imaging and Research, Copenhagen University Hospital Hvidovre, Denmark. All experiments were performed at the Danish Research Centre for Magnetic Resonance.

### **Chair person**

PhD, DM, DMSc. Jens Dahlgaard Hove

### **Review committee**

Professor, MD, DMSc. Hans Stødkilde Jørgensen

Professor, PhD. Damian Tyler

### **Funding**

The studies in this PhD thesis were supported by grants from The Spies Foundation, The Lundbeck Foundation, The Danish Heart Association and Copenhagen University Hospital Hvidovre.

## Acknowledgements

First of all I would like to express my great appreciation to my supervisor Per Åkeson for given me the opportunity to do research within the field of hyperpolarized  $^{13}\text{C}$  MRS. This would not have been possible without the support from Olaf B. Paulson, who as a former leader at DRCMR believed in the technique and saw the opportunities for the department to expand the research area in this brand new and exciting direction. I would also like to thank Per Åkeson for sharing me his great knowledge and for pushing me forward and making me keep my focus, when the experiments did not go my way.

I would like to thank my project supervisors Peter Magnusson and Lise Vejby Søgaard, for guidance through the complicated area of MR. Peter for his persistent help with improving the experimental setup and imaging analysis. Lise for keeping things running when needed, for our great scientific discussions and for her warm and caring personality.

Importantly, I would like to express my gratitude to Jan Henrik-Ardenkjær Larsen for becoming my supervisor, for his enormous inspiration and drive as a scientist and person, and for sharing his limited time for me and my ideas.

A special thank goes to Sascha Gude, for her help with the animals and for making me want to show up for work before the birds get up. I would also like to thank my colleges and office bodies Sadia Asgar Butt and Christoffer Laustsen. Sadia for her great laughter and inspiring ideas and Christoffer for his bright analytical mind, his great stories and his funny and relaxed personality.

Finally, I would like to thank my family and friends, especially Bjarke and his family for all their love and support when I needed it the most.

## Resumé

Iskæmisk hjerte sygdom er en alvorlig sygdom med høj mortalitet specielt i den vestlige verden. Sygdommen er karakteriseret ved forsnævring af kranspulsåren, der hæmmer tilførslen af ilt til en større eller mindre del af hjertet.

Ændringer i hjertes energimetabolisme er en kendt effekt af iskæmi. Formålet med denne afhandling var at undersøge, hvorvidt hyperpolariseret magnetisk resonans (MR) med kulstof  $^{13}\text{C}$ -mærket pyruvat kunne bruges i rotter til at detektere og visualisere ændringer i hjertets metabolisme. Teknikken blev først etableret og optimeret i raske rotter. Ved i.v. indsprøjtning af hyperpolariseret  $[1-^{13}\text{C}]$ pyruvat kunne omdannelsen af  $[1-^{13}\text{C}]$ pyruvat i hjertemusklen følges med MR. Signal fra det indsprøjtede  $[1-^{13}\text{C}]$ pyruvat blev primært observeret fra blodet inde i ventriklerne, hvorimod signal fra dets metabolitter  $[1-^{13}\text{C}]$ laktat,  $[1-^{13}\text{C}]$ alanin og  $[1-^{13}\text{C}]$ bikarbonat blev observeret i hjertemusklen tættest på spolen. Teknikken blev derefter afprøvet i to studier. Ved en operation blev rottens kranspulsåre afsnøret i 30 minutter efterfulgt af 2 times reperfusion. Rotterne blev scannet med hyperpolariseret  $[1-^{13}\text{C}]$ pyruvat før og efter operationen. Et tydeligt fald i signal fra  $[1-^{13}\text{C}]$ laktat og  $[1-^{13}\text{C}]$ alanin kunne observeres i det iskæmiske område efter operationen i forhold til før operationen. Alvorligheden af iskæmien blev verificeret med gadolinium-baseret late enhancement imaging, som viste øget signal fra det iskæmiske område. Desuden sås der øget niveau af hjerteinfarkt markøren Troponin I. I forhold til før operationen, var det ikke muligt at opfange signal fra  $[^{13}\text{C}]$ bikarbonat i hjertet efter operationen. Vores hypotese var at det skyldes en hæmning af enzymet PDH, som omdanner  $[1-^{13}\text{C}]$ pyruvat til acetyl-CoA og  $[^{13}\text{C}]$ bikarbonat i hjertecellerne.

I det efterfølgende studie undersøgte vi muligheden for at øge signalet fra  $[^{13}\text{C}]$ bikarbonat ved infusion af glukose, insulin og kalium (GIK) i fastede rotter, hvor man ved at PDH aktiviteten er lav. To forskellige doser blev testet, en høj og en lav. Signifikant øget  $[^{13}\text{C}]$ bikarbonat signal kunne detekteres i højdosisgruppen i forhold til den fastede tilstand, hvilket indikerer at GIK kan øge hjertets forbrug af glukose som energikilde ved at øge flux af pyruvat gennem PDH.

Disse to studier antyder at hyperpolariseret magnetisk resonans med  $[1-^{13}\text{C}]$ pyruvat kan bruges i rotter til at til at detektere og visualisere ændringer i hjertet metabolisme. Resultaterne fra studierne under PhD-forløbet har resulteret i to artikler. En som er publiceret og en som er submittet. Artiklerne er vedhæftet sidst i afhandlingen.

## Summary

Ischemic heart disease is one of the leading causes of death in the western countries. The disease is characterized by narrowing of the coronary arteries, which limits oxygen supply to the myocardium. Early in the development of the disease, changes in the myocardial metabolism can be observed. Hyperpolarized magnetic resonance spectroscopy (MRS) using  $^{13}\text{C}$  labelled pyruvate is a newly developed technique, which can detect and visualize myocardial metabolism. The aim of the thesis was to examine if hyperpolarized  $[1-^{13}\text{C}]$ pyruvate MRS could be used to assess changes in myocardial metabolism in rats in vivo. The technique was first established and optimized in healthy rats and then evaluated in two studies. First in a rat model of severe myocardial ischemia and then in rats given an infusion of glucose, insulin and potassium (GIK).

In the first study, after i.v. injection of  $[1-^{13}\text{C}]$ pyruvate, metabolic images of the  $[1-^{13}\text{C}]$ pyruvate metabolites  $[1-^{13}\text{C}]$ lactate,  $[1-^{13}\text{C}]$ alanine and  $[1-^{13}\text{C}]$ bicarbonate was observed the healthy rat hearts. The signal from  $[1-^{13}\text{C}]$ pyruvate was primarily observed from the blood inside the ventricles, whereas the signal from  $[1-^{13}\text{C}]$ lactate,  $[1-^{13}\text{C}]$ alanine and  $[1-^{13}\text{C}]$ bicarbonate was confined to the anterior myocardial wall closest to the coil. By a surgical procedure the left anterior descending artery was occluded for 30 min followed by 2 hours of reperfusion. After ischemia a decrease in the signal from  $[1-^{13}\text{C}]$ lactate and  $[1-^{13}\text{C}]$ alanine was observed in at the region of ischemia compared to before ischemia. The severity of the ischemic insult was verified by increased Troponin I blood levels and gadolinium-based late enhancement imaging, which showed enhanced signal in the ischemic region.

Signal from  $[1-^{13}\text{C}]$ bicarbonate was under the limit of detection after ischemia, and could therefore not be assess. We hypothesised that the low  $[1-^{13}\text{C}]$ bicarbonate signal post-ischemia could be due to an overall depression of the flux of pyruvate through the PDH enzyme.

In the second study we wanted to test, if it was possible to increase the PDH-flux in fasted rats, seen as an increase of  $[^{13}\text{C}]$ bicarbonate signal in the myocardium, by injection of glucose, insulin and potassium (GIK). Two doses of GIK were tested a high dose and a low dose. Significant increase in  $[^{13}\text{C}]$ bicarbonate signal was observed after GIK-infusion in the high dose group compared to fasted, indicating an increased glucose oxidation and increased flux of pyruvate through PDH.

Thus, these two studies suggest that hyperpolarized  $[1-^{13}\text{C}]$ pyruvate MRS can be used to assess changes in myocardial metabolism in rats in vivo. The results were presented in two papers. One published and the one submitted. Both added as appendixes to this thesis.



## Prologue

During the second half of the twentieth century diagnostic methods to assess ischemic heart disease have successfully improved, resulting in a significant reduction in mortality especially in the industrialized world. In respect to this, advanced non invasive imaging techniques have played an important role. Magnetic resonance imaging (MRI) is one of these techniques, which have been established and implemented in the clinical routine, and is now considered the gold standard for assessing cardiac autonomy, function and mass. MRI is also frequently used to evaluate myocardial perfusion and viability with gadolinium-based contrast agents. However, the development of new improved imaging techniques will lead to improvements of both disease diagnosis and understanding. Recently research in cardiac metabolism has gained a lot of focus, since metabolic alterations are suggested to be an early marker of disease. Hyperpolarized  $^{13}\text{C}$  MRS is a newly developed magnetic resonance spectroscopy technique, which can detect and visualize cardiac metabolism. In this PhD thesis hyperpolarized  $^{13}\text{C}$  MRS were evaluated to assess changes in cardiac metabolism.

The data obtained during the PhD period form the basis of two papers.

### Paper I:

*Imaging regional metabolic changes in the ischemic rat heart in vivo using hyperpolarized  $[1-^{13}\text{C}]$ Pyruvate*

Lauritzen et al. NMR in Biomedicine 2013 [published]

### Paper II:

*Enhancing the  $[^{13}\text{C}]$ bicarbonate signal in cardiac hyperpolarized  $[1-^{13}\text{C}]$ pyruvate MRS studies by infusion of glucose, insulin and potassium*

Lauritzen et al. Circulation: Cardiovascular Imaging [submitted]

### Thesis outline

As introduction, a review of the current knowledge of cardiac metabolism is presented in relation to cardiac ischemia, as well as an overview of the recent interventions to improve diagnosis and outcome for patients with ischemic heart disease. In this perspective, conventional cardiac MRI and recent studies with hyperpolarized  $[1-^{13}\text{C}]$ pyruvate MRS is reviewed. The methodological approaches relevant to this thesis is shortly presented. The main results are summarized. The data obtained are discussed in relation to other studies in the research field. Lastly, a conclusion and perspectives for future applications of the technique are discussed.

## List of Abbreviations

ALT	Alanine Aminotransferase	LE	Late Enhancement
ATP	Adenosine Triphosphate	LP	Line Profile
CA	Carbonic Anhydrase	MR	Magnetic Resonance
CI	Confidence Interval	MRI	Magnetic Resonance Imaging
CSI	Chemical Shift Imaging	MRS	Magnetic Resonance Spectroscopy
DCA	Dichloroacetic Acid	NADH	Nicotinamide Adenine - Dinucleotide Hydride
DNP	Dynamic Nuclear Polarization	PET	Position Emission Tomography
ECG	Electrocardiogram	PDK	Pyruvate Dehydrogenase Kinase
EDTA	Ethylenediaminetetraacetic Acid	PDP	Pyruvate Dehydrogenase - Phosphatase
FAT	Fatty Acid Translocase	PDH	Pyruvate Dehydrogenase
FFA	Free Fatty Acids	RF	Radio Frequency
FOV	Field Of View	SNR	Signal to Noise Ratio
Gd	Gadolinium	SPECT	Single Photon Emission Computed Tomography
GTP	Guanosine Triphosphate	TCA	Tricarboxylic Acid Cycle
GIK	Glucose, Insulin and Potassium	TE	Echo Time
HSVD	Hankel Singular Values - Decomposition	TRIS	Tris(hydroxymethyl) - aminomethane
IHD	Ischemic Heart Disease	TR	Repetition Time
LAD	Left Anterior Descending- Coronary Artery		
LDH	Lactate Dehydrogenase		

## TABLE OF CONTENTS

<b><u>PROLOGUE</u></b> .....	<b>8</b>
<b><u>LIST OF ABBREVIATIONS</u></b> .....	<b>9</b>
<b><u>TABLE OF CONTENTS</u></b> .....	<b>10</b>
<b><u>INTRODUCTION</u></b> .....	<b>11</b>
Ischemic heart disease .....	11
Myocardial energy metabolism .....	12
Cardiac MRI .....	14
MR contrast agents for assessment of myocardial ischemia .....	15
Magnetic resonance spectroscopy (MRS) .....	16
Hyperpolarization – The DNP method .....	16
Hyperpolarized [1- <sup>13</sup> C]pyruvate MRS .....	17
<b><u>AIM &amp; HYPOTHESIS</u></b> .....	<b>19</b>
<b><u>METHODS</u></b> .....	<b>20</b>
Animal model of LAD occlusion .....	20
GIK infusion .....	21
[1- <sup>13</sup> C]pyruvate sample preparation .....	21
MR system and hardware .....	21
Anatomical MRI and late enhancement .....	21
Chemical shift imaging .....	22
Evaluation of Troponin I and blood glucose levels .....	22
MRS analysis .....	22
Statistics .....	23
<b><u>MAIN RESULTS</u></b> .....	<b>25</b>
Paper I .....	25
Paper II .....	29
<b><u>DISCUSSION</u></b> .....	<b>32</b>
<b><u>CONCLUSION AND PERSPECTIVES</u></b> .....	<b>35</b>
<b><u>REFERENCES</u></b> .....	<b>37</b>

**Paper I:** Lauritzen et al. Circulation: Cardiovascular Imaging [submitted]

**Paper II:** Lauritzen et al. NMR in Biomedicine. 2013 [published]

## **Introduction**

### **Ischemic heart disease**

Ischemic heart disease (IHD) is one of the leading causes of death in the western countries. World wide more than 42 million people suffer from IHD, which has become a major public health burden (1). A high fat and energy-rich diet, smoking and a sedentary life-style are associated with the emergence of IHD. With the urbanization of the developing world, the prevalence of risk factors such as obesity, insulin resistance and type 2 diabetes, a large increase in IHD is projected and the disease is likely to become the most common cause of deaths worldwide by 2020 (1). Myocardial ischemia is characterized by a situation, which the blood and oxygen supply to the heart tissue are not sufficient to meet its metabolic needs. The most common underlying cause is narrowing of coronary arteries by atherosclerosis. In atherosclerosis lipoprotein accumulates in the cardiovascular wall resulting in a reduction in the arterial lumen and stiffness of the wall. This limits the vessels ability to dilate and increase blood flow when oxygen demands increases during increased cardiac work. Acute obstruction or persistent impairment in blood flow can lead to irreversible cell damage (necrosis). This condition is referred to as myocardial infarction. A large infarct can cause disturbances in the mechanical, biochemical and electrical functions of the myocardium, which may lead to heart failure or trigger life threatening arrhythmias. There has therefore been an increased interest in characterizing disease progression, and identifying interventions that are able to reduce the myocardial infarct area and improve cardiac function in patients with IHD.

Today diagnosis of IHD depends predominately on patient symptoms, such as chest pain and/or shortness of breath, electrocardiographic features and assessment of cardiac blood markers. The most commonly used blood markers for myocardial infarction is creatin kinase (CK-MB), Troponin T/I and bran naturetic Peptide (BNP), which can be detected in the blood after an ischemic episode (2). However, several others bio markers exist and are often measured in combination with each other to increase the diagnostic sensitivity (3). Troponin I is currently the only biomarker, which is cardio specific. It is released to the blood stream only in response to myocardial tissue damage (2). An echocardiogram (ECG) gives information on the electrical properties of the heart. If the patients have a ST-segment elevation (or depression), it can be a sign of infarction. If the patient is presented with all of the above findings, the patient will almost immediately be directed to revascularization (opening of the obstructed vessel by balloon angioplasty or stenting). This is performed during an X-ray based coronary angiography, which can reveal where the obstruction is located and guide the physician when performing the revascularization. However, diagnosis of patients with nonspecific symptoms and no ECG changes or no abnormalities observed during angiography can be difficult to diagnose. A recent study has shown that up to 50% of the patients who arrives to the hospital with chest pain, is found non-diagnostic with no significant changes in the ECG (3, 4). In these situations the patient is directed to further examination by coronary CT, MRI or PET/SPECT scanning.

## Myocardial energy metabolism

Proper heart function requires a constant high energy production and is dependent on a high O<sub>2</sub> supply to produce enough energy to maintain the essential cellular processes. 95% of the ATP production comes from oxidative phosphorylation in the mitochondria with the remaining from glycolysis and GTP formation in the citric acid cycle (TCA cycle). The heart differs from other tissues in that it has a unique ability regulate its substrate usage at different levels to fulfill its energy requirement. Under normal healthy conditions the heart utilizes mainly free fatty acids (FFA) for ATP production (40-60%), with little contribution from glucose (20-10%) and the remaining from lactate, amino acids and ketone bodies. During an overnight fast the heart can increase its FFA utilization up to 90% (5, 6).

Glucose transport into the cardiomyocytes is regulated by the transmembrane glucose gradient and by the content of glucose transporters (GLUT-4 and GLUT-1) in the sarcolemma. The translocation of GLUT-4 and GLUT-1 from intracellular vesicles to the sarcolemma membrane is regulated by several factors such as insulin stimulation, and increased cardiac work demand (7). Upon uptake, glucose is phosphorylated to glucose 6-phosphate by hexokinase, and then further converted to pyruvate through glycolysis in the cytosol. Here pyruvate is converted to lactate by the enzyme lactate dehydrogenase (LDH) and alanine via the enzyme alanine aminotransferase (ALT). In the mitochondrial membrane pyruvate is converted to acetyl-CoA by the pyruvate dehydrogenase (PDH) enzyme complex. Acetyl-CoA then enters the TCA cycle for generation of energy (figure 1). The activity of the PDH enzyme is tightly regulated. PDH is inactivated by PDH-kinase (PDK) and reactivated by PDH-phosphatase (PDP). High intra-mitochondrial concentration of acetyl-CoA and NADH stimulates PDK, resulting in PDH inhibition (negative feedback) (8, 9).

FFA's are released into the blood from adipose tissue and hepatic triglyceride stores. FFA enters the cardiomyocytes either by passive diffusion or by protein-mediated transport involving either the fatty acid translocase (FAT) or the plasma membrane fatty acid binding protein (FABP) (10). FFA's are also converted to acetyl-CoA via mitochondrial  $\beta$ -oxidation and thereby compete with glucose for entering the TCA cycle via acetyl-CoA. In situations of fasting, where the blood glucose level is low, FFA lipolysis increases, PDH is inactivated and the FFA oxidation increases. In contrast, insulin is known to stimulate PDP thereby reactivating PDH and inhibiting FFA metabolism. Insulin also stimulates glucose uptake and increases glycolysis, which leads to increased levels of pyruvate that inhibits PDK and thereby stimulates PDH indirectly (8, 11, 12). The healthy non-ischemic human heart is a net consumer of lactate and has shown to be an important source of pyruvate formation even under conditions of high cardiac power (13).

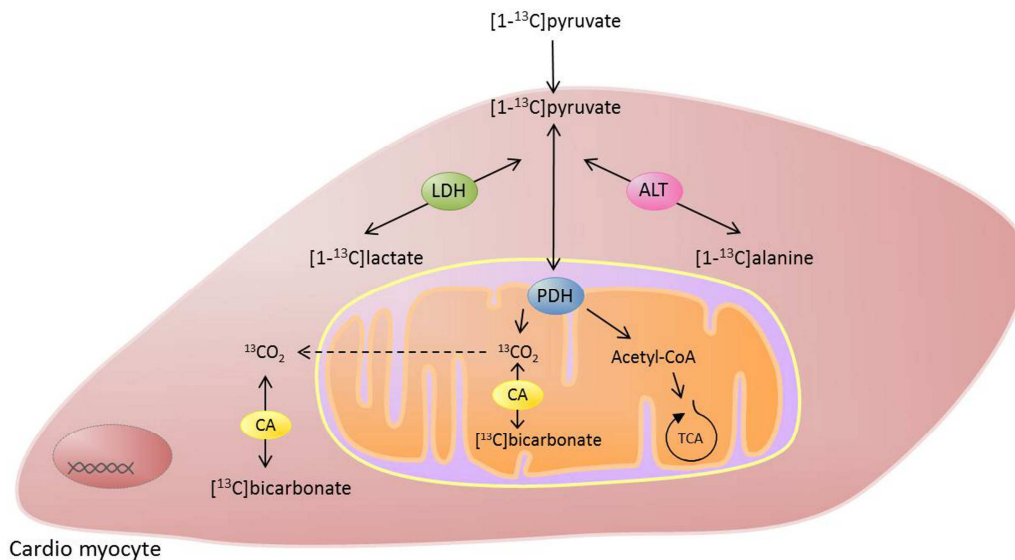


**Figure 1.** When injected i.v. [1-<sup>13</sup>C]pyruvate is taken up by the cardio-myocytes and converted into [1-<sup>13</sup>C]lactate via the enzyme lactate dehydrogenase (LDH) and [1-<sup>13</sup>C]alanine via alanine aminotransferase (ALT) in the cytosol. [1-<sup>13</sup>C]pyruvate is also converted into Acetyl CoA via the pyruvate dehydrogenase (PDH) complex in the mitochondrial membrane. In the process [<sup>13</sup>C]bicarbonate is produced via <sup>13</sup>CO<sub>2</sub> and the enzyme carbonic anhydrase (CA). Acetyl CoA is one of the main fuels for production of energy in the TCA-cycle.

The pattern of substrate uptake and utilization has shown to change in different cardiac diseases, such as heart failure and IHD. During ischemia a metabolic shift towards glucose relative to FFA has shown to represent an adaptation to a lower oxygen environment in poorly perfused areas of the myocardium, due to the fact that less oxygen is required for glucose oxidation per unit ATP produced compared to FFA oxidation (14). The metabolic consequences of myocardial ischemia includes, increased glycogen breakdown and increased glucose uptake followed by increasing anaerobic glycolysis with increased lactate production, a decrease in mechanical work and a decreased TCA cycle activity due to the decreasing oxygen availability. Despite of this, it has been shown that the majority of the acetyl-CoA during mild to moderate ischemia (20-30% reduction in coronary blood flow) still derives from FFA  $\beta$ -oxidation (15, 16). Furthermore a reduction in PDH-flux is observed (17). Whether the reduction is due to a direct effect by increased phosphorylation and inhibition of the PDH enzyme, or an indirect effect by a build up of NADH and acetyl-CoA in the mitochondria, is still under discussion.

In patients with acute myocardial infarction a rapid rise in plasma FFA are observed in the first 1-2 hours after onset of symptoms (18). The elevated level of FFA is believed to worsen the ischemic damage of the myocardium (19). Infusion of glucose, insulin and potassium (GIK), is able to decrease the circulating FFA levels and increase glucose uptake and utilization, which have shown to have a direct protective effect on ischemic tissue (20). In positron emission tomography (PET) studies GIK infusions have shown to increase the uptake of the radioactive fluorine-18 labelled glucose analogue, [<sup>18</sup>F]FDG, to maintain a metabolic steady state during

scanning and improve image quality (21, 22), whereas fasting prior to PET scanning have shown heterogeneous [ $^{18}\text{F}$ ]FDG uptake and poor image quality (23, 24). As described above insulin is also known to increase flux through PDH. GIK infusions have therefore been extensively studied as a therapy in patients with myocardial infarction (25, 25). Other drugs known to inhibit FFA oxidation have also been studied as treatment for myocardial ischemia. One of these is dichloroacetate (DCA), which act primarily by increasing pyruvate oxidation by inhibiting PDK, thus preventing phosphorylation of PDH (26). Additionally, DCA has shown to stimulate glucose and lactate oxidation in the anaerobic heart and improve cardiac function after ischemia (27). DCA is also suggested to inhibit FFA oxidation by shuttling acetyl-CoA out of the mitochondria (28). Several other drugs known to decrease FFA oxidation and increase glucose oxidation in the myocardium have recently been developed and tested against myocardial ischemia (29, 30). However their mechanism of action is beyond the scope of this thesis.

## Cardiac MRI

The following section will give a short introduction to cardiac MRI. For further information on the basic principles of MRI the reader is referred to textbooks on this subject (e.g Brown and Semelka 2003) (31).

Conventional MRI is based on the magnetic properties of protons ( $^1\text{H}$ ), which are the most abundant atomic nuclei in our body in the form of water. When the human body is placed in a MR-scanner the orientation of the protons aligns with the magnetic field. In order to obtain signal from the protons in our body and create images, short radiofrequency (RF) pulses can be applied. If applied in the same frequency as the protons, they absorb the energy and start to rotate within the magnetic field. How much they rotate depends on the power of the RF pulse. When the RF pulse is turned off the rotation returns back to its equilibrium along the magnetic field. In the process energy is released. The emitted energy signal can be detected by specific RF-coils. The time of which the magnetization of the excited protons returns to its equilibrium is called relaxation (or decay), which are characterized by two time constants T1 and T2. The decay depends on the tissue type the protons are situated in and the surrounding magnetic environment. This is exploited in MRI to produce detailed images of the human body with exceptional well soft tissue contrasts e.g. between fat and water (31, 32)

MRI offers a comprehensive morphological and functional evaluation of the heart, because of its soft tissue contrast capabilities. It provides good spatial and temporal resolution, and is therefore now considered the gold standard for assessing ventricular mass and volume as well as regional wall motion abnormalities (33). However, cardiac MRI also poses a number of imaging challenges. For good quality images to be obtained motion artifacts has to be compensated for by e.g. cardiac and respiratory gating. Cardiac gating is performed by measuring the ECG signal. Usually the R-wave (the highest pulse in the ECG signal) is used for gating. ECG can be combined with respiratory gating. Sometimes the respiratory movement can be registered in the ECG itself or it can be measured externally and combined with the ECG signal. MR acquisition

is then performed in between the greatest movements. However, gating is time consuming, so in healthy subjects breath-holding is normally performed to avoid prolonged MR-acquisitions. Cine imaging is a standard cardiac imaging technique, which uses the gating signal to obtain multiple images at one slice position during the R-R time interval. Rapid display of these images allows a dynamic visualization of the heart during different phases of the heart cycle, which can be used to measure ventricular dimensions and/or detect wall motion deficiencies (34).

## **MR contrast agents for assessment of myocardial ischemia**

The MR signal can be enhanced by different chemical compounds, which are injected i.v. Magnevist® (gadopentetate dimeglumine) and Dotarem® (gadoterate meglumine) consist of gadolinium (Gd), a paramagnetic metal and a stable chelate: DTPA or DOTA respectively. Both contrast agents are used worldwide for clinical purposes. The contrast agents has the unique properties of shortening the T1-relaxation and is therefore easily detected using T1 sensitive image sequences (33). In patients with IHD the contrast agents can be used to assess myocardial perfusion, to quantify extension of myocardial infarction, to differentiate between occluded and reperfused infarcts and to determine potential viability of the tissue. Due to wash-in wash-out differences between normal and ischemic myocardium increased signal intensity from the contrast agent can be detected in the ischemic area compared to the surrounding healthy heart tissue. This is usually referred to as late enhancement (LE) imaging, because the images are obtained between 10-20 min after i.v. administration of the contrast agent. When the entire left ventricle is covered by series of short axis slices, quantification of the infarct size is possible (35). This is done by measuring the enhanced areas on every slice calculating the total infarcted mass of the left ventricle. LE is also used to assess viability. Subendocardial or absent enhancement patterns have a high positive predictive value for viability, while homogenous transmural enhancement correlates with the absence of functional recovery in only nearly half of infarct segments and finally the pattern of signal enhancement surrounding a region without signal is exclusively associated with the absence of viability (36). Monitoring of the early distribution of the contrast agent (1-2 min) after administration is another technique called the “first pass” technique. This technique highlights the differences in the enhancement of normal and underperfused myocardial regions (37). However, both the LE imaging technique, the viability measurements and the “first pass” perfusion technique, are still being discussed by means of their clinical values in relation to other well documented diagnostic imaging techniques/methods such as PET and CT. The location and extent of acute and subacute infarction can also be visualized using T2-weighted images, since formation of interstitial edema increases the T2-relaxation time (38). However, T2 sequences often induce flow artifacts in cardiac studies (due to the long TR and TE required).

## **Magnetic resonance spectroscopy (MRS)**

MRS differs from conventional MRI in that it offers the possibility of studying the chemical composition of tissues and to follow biochemical processes non-invasively. The underlying principle of MRS is that all atomic nuclei are surrounded by a cloud of electrons, which affect the local magnetic field in which the nucleus is immersed. The surrounding nearby nuclei also affects the magnetic field contributing to a change in the magnetic environment referred to as a diamagnetic effect or a chemical shift. This can be measured by MR as difference in resonance frequency expressed by parts per million (ppm). The different signals from the chemical composition of the tissue are shown as a 'spectra' and the individual chemicals can be quantified by measuring the area under the curve for each peak in the spectra. While theoretically possible on any MRI system MRS has several limitations, which has limited its widespread acceptance in routine clinical practice, MRS can detect signal from different atomic nuclei such as  $^1\text{H}$ ,  $^{13}\text{C}$ ,  $^{23}\text{N}$  and  $^{31}\text{P}$ . However, compared to  $^1\text{H}$  the MR sensitivity of other nuclei is low, due to low in vivo abundance and has therefore primarily been used for research (39). In cardiac research  $^1\text{H}$  and  $^{31}\text{P}$  MRS have been of particular interest.  $^1\text{H}$  MRS has been used to detect signal from e.g. myocardial fat, lactate, creatine in the heart (40-42).  $^{31}\text{P}$  MRS has primarily been used to detect compounds involved in energy metabolism such as ATP and phosphocreatine (43, 44). MRS is a common single-voxel technique, but multi-voxel MRS techniques have been developed. One well established technique is chemical shift imaging (CSI), which enables construction of metabolic images from the acquired MRS signal from several voxels (45). Usually a 2D sequence is used, but the spatial encoding is possible in all three spatial dimensions (46).

## **Hyperpolarization – The DNP method**

Hyperpolarization MRS makes it possible to study biochemical processes that are normally too low of in vivo abundance to be studied by conventional MRS alone. Hyperpolarization refers to a condition, which polarization (magnetization) of a specific nucleus is enhanced beyond its normal thermal equilibrium. Using the dissolution-dynamic nuclear polarization (DNP) method biological relevant compounds are hyperpolarized in a polarizer outside the imaging system for to be rapidly diluted in a solvent, quickly transported to the scanner, injected and imaged (47). The method takes advantage of the fact that polarization of electrons can be transferred to the nuclear spins in the solid state. This is done by adding microwave radiation to the sample in a frequency close to the resonance frequency of the electron spin. Normally  $^1\text{H}$ ,  $^{13}\text{C}$  or  $^{15}\text{N}$  nuclear labelled compound are used because these nucleus have highly polarized nuclear spins. In order to achieve full polarization unpaired electron spins are added to the sample. Organic radicals such as nitroxides or trityls are often used as sources for unpaired electrons, because they are chemically stable, hydrophilic and well tolerated in vivo. The sample containing the labelled nucleus is transferred to a high magnetic field (3.35-5T) inside the polarizer and rapidly lowered into liquid helium. In this solid frozen state the electron spins become highly polarized. By microwave radiation the electron polarization is transferred to the lower polarized nuclear spins.

This takes between 30-60 min. After the polarization the sample is melted and dissolved by a heated buffer inside the polarizer without losing the polarization. However once outside the polarizer the compound loses its polarization relatively fast (within minutes), due to T1-relaxation. Therefore the solvent has to be injected very rapidly i.v. after dissolution in order to keep the polarization as high as possible (47, 48). When injected the biological compound is taken up by the cells and the spatial distribution of the hyperpolarized labelled nucleus can be followed through several steps in metabolic pathways, adding information of specific enzymatic flux rates (49-51). In this thesis 1-<sup>13</sup>C labelled pyruvate was used. However, many molecules involved in cellular metabolism can be hyperpolarized, making it possible to follow different metabolic pathways and enzymatic flux rates in vivo (table 1).

Dissolution-DNP Compounds (97–106)

Agent	Products
[1- <sup>13</sup> C]pyruvate	[1- <sup>13</sup> C]lactate, [1- <sup>13</sup> C]alanine, [ <sup>13</sup> C] bicarbonate, <sup>13</sup> CO <sub>2</sub>
[2- <sup>13</sup> C]pyruvate	[2- <sup>13</sup> C]lactate, [2- <sup>13</sup> C]alanine, [1- <sup>13</sup> C]acetyl-carnitine, [1- <sup>13</sup> C]citrate, [5- <sup>13</sup> C]glutamate
[1,2- <sup>13</sup> C <sub>2</sub> ]pyruvate	[1,2- <sup>13</sup> C <sub>2</sub> ]lactate, [1,2- <sup>13</sup> C <sub>2</sub> ]alanine, [1- <sup>13</sup> C]acetyl-carnitine, [1- <sup>13</sup> C]citrate, [5- <sup>13</sup> C]glutamate, [ <sup>13</sup> C]bicarbonate, <sup>13</sup> CO <sub>2</sub>
[1- <sup>13</sup> C]actate	[1- <sup>13</sup> C]pyruvate, [1- <sup>13</sup> C]alanine, [ <sup>13</sup> C] bicarbonate, <sup>13</sup> CO <sub>2</sub>
<sup>13</sup> C-bicarbonate	<sup>13</sup> CO <sub>2</sub>
[1,4- <sup>13</sup> C <sub>2</sub> ]fumarate	[1,4- <sup>13</sup> C <sub>2</sub> ]malate
[1- <sup>13</sup> C]acetyl-methionine	[1- <sup>13</sup> C]methionine
[2- <sup>13</sup> C]fructose	[1- <sup>13</sup> C]fructose-6-phosphate
[5- <sup>13</sup> C]glutamine	[5- <sup>13</sup> C]glutamate
[1- <sup>13</sup> C]ethylpyruvate	[1- <sup>13</sup> C]pyruvate, [1- <sup>13</sup> C]lactate, [1- <sup>13</sup> C]alanine, [ <sup>13</sup> C] bicarbonate, <sup>13</sup> CO <sub>2</sub>
[1,1- <sup>13</sup> C <sub>2</sub> ]acetic anhydride	Multiple depending on reactant
[1- <sup>13</sup> C]acetate	[1- <sup>13</sup> C]acetyl-carnitine
<sup>13</sup> C Urea	None
bis-1,1-(hydroxymethyl)-[1- <sup>13</sup> C]cyclopropane-d8 HP001	None
α-keto-[1- <sup>13</sup> C]isocaproate	[1- <sup>13</sup> C]leucine
[1- <sup>13</sup> C]dehydro ascorbic acid	[1- <sup>13</sup> C]ascorbic acid
[1- <sup>13</sup> C]alanine	[1- <sup>13</sup> C]lactate, [1- <sup>13</sup> C]pyruvate, [ <sup>13</sup> C]bicarbonate

**Table 1.** List of <sup>13</sup>C labelled compounds that have been hyperpolarized by the dissolution-DNP method. Hurd et al. 2012 (48).

## Hyperpolarized [1-<sup>13</sup>C]pyruvate MRS

As motioned above hyperpolarized [1-<sup>13</sup>C]pyruvate was used in this thesis to study cardiac metabolism. Pyruvate is biologically interesting because it is the end product of the glycolysis and one of the main fuels for formation of acetyl-CoA, which enters the TCA cycle for generation of energy (ATP). By i.v. injection hyperpolarized [1-<sup>13</sup>C]pyruvate is taken up by the myocytes and, as described above, converted into [1-<sup>13</sup>C]lactate via the enzyme LDH and [1-<sup>13</sup>C]alanine via the enzyme ALT. Both enzymes are located in the cytosol. Furthermore, [1-<sup>13</sup>C]pyruvate is converted in to acetyl-CoA via the PDH enzyme complex in the mitochondrial membrane. In this process the <sup>13</sup>C-atom in the C-1 position of the pyruvate molecule is transferred to <sup>13</sup>CO<sub>2</sub> in equilibrium with [<sup>13</sup>C]bicarbonate via the enzyme carbonic anhydrase

(CA) (17, 50, 52). However, often only [1-<sup>13</sup>C]lactate, [1-<sup>13</sup>C]alanine and [<sup>13</sup>C]bicarbonate and not <sup>13</sup>CO<sub>2</sub> can be detected with hyperpolarized MRS in vivo, due to sensitivity, since the equilibrium at physiological pH is highly shifted towards bicarbonate. The production of [<sup>13</sup>C]bicarbonate is suggested to reflect the mitochondrial status, whereas production of [1-<sup>13</sup>C]lactate and [1-<sup>13</sup>C]alanine is suggested to reflect the general metabolic state of the myocytes, according to the location of the different enzymes in the cell (53) (Figure 1).

Application of hyperpolarized <sup>13</sup>C MRS for evaluation of myocardial ischemia has been demonstrated in animals recently (17, 53-56). Experiments performed in isolated rat hearts have shown that hyperpolarized [1-<sup>13</sup>C]pyruvate MRS can detect the metabolic consequences of ischemia. In the study by Schroeder et al. decreased [<sup>13</sup>C]bicarbonate signal and increased [1-<sup>13</sup>C]lactate signal were detected after 10 minutes of global myocardial ischemia, indicating a decreased PDH-flux and increased anaerobic lactate formation via the LDH enzyme (17). Hyperpolarized [1-<sup>13</sup>C]pyruvate MRS has also been used to generate metabolic images in pigs with myocardial ischemia (53, 57). In the study by Golman et al. the left anterior descending coronary artery (LAD) was occluded for 15 minutes (mild ischemia) or 45 minutes (severe ischemia) respectively, followed by 2 hours of reperfusion. Metabolic maps of the [1-<sup>13</sup>C]pyruvate metabolites showed decreased PDH-mediated [<sup>13</sup>C]bicarbonate production after 15 minutes occlusion in the ischemic region of the myocardium. After 45 minutes occlusion both production of [<sup>13</sup>C]bicarbonate and [1-<sup>13</sup>C]alanine was decreased in the ischemic region representing a depression of both the mitochondrial activity and the overall cellular activity. The metabolic images were compared with gadolinium-based LE images, which showed enhanced signal after 45 min occlusion, but no changes after 15 min occlusion. The study demonstrates how hyperpolarized <sup>13</sup>C MRS can detect and visualize metabolic changes even during mild ischemic conditions in the heart, before other MR methods such as LE imaging reveals any abnormalities.

The effect of fasting on hyperpolarized <sup>13</sup>C MRS signal has recently been examined in vivo by Schroeder et al. (51) Low myocardial [<sup>13</sup>C]bicarbonate signal was observed in fasted rats after [1-<sup>13</sup>C]pyruvate injection compared to fed rats, indicating a low flux of [1-<sup>13</sup>C]pyruvate through PDH. Furthermore, hyperpolarized <sup>13</sup>C MRS studies in perfused hearts have shown that hearts exposed to substrates mimicking a fasted state resulted in a 60 % reduction of [1-<sup>13</sup>C]pyruvate utilization compared to a fed state (58). These studies stress the importance of ensuring a fed condition when measuring cardiac metabolism with hyperpolarized [1-<sup>13</sup>C]pyruvate.

## **Aim & Hypothesis**

### Overall aim

The overall aim of the thesis was to examine if hyperpolarized magnetic resonance imaging could be used to assess changes in myocardial metabolism in rats in vivo. This was examined in the following two papers.

### **Paper I:**

*Imaging regional metabolic changes in the ischemic rat heart in vivo using hyperpolarized [1-<sup>13</sup>C]Pyruvate*

#### **Aim**

The aim of Paper I was to investigate if hyperpolarized [1-<sup>13</sup>C]pyruvate MRS could be used to visualize regional changes in the myocardial metabolism in an in vivo rat model of acute myocardial ischemia.

#### **Hypothesis:**

The hypothesis was that changes in the signal from the [1-<sup>13</sup>C]pyruvate metabolites [1-<sup>13</sup>C]lactate, [1-<sup>13</sup>C]alanine and [<sup>13</sup>C]bicarbonate could be visualized regionally in the ischemic rat heart using hyperpolarized [1-<sup>13</sup>C]pyruvate MRS imaging.

### **Paper II:**

*Enhancing the [<sup>13</sup>C]bicarbonate signal in cardiac hyperpolarized [1-<sup>13</sup>C]pyruvate MRS studies by infusion of glucose, insulin and potassium*

#### **Aim:**

The aim of Paper II was to investigate if infusion of glucose, insulin and potassium (GIK), could increase the [<sup>13</sup>C]bicarbonate signal in cardiac hyperpolarized [1-<sup>13</sup>C]pyruvate MRS measurements in fasted rats.

#### **Hypothesis:**

The hypothesis was that infusion of GIK could increase the myocardial glucose oxidation and flux of pyruvate through PDH seen as an increase of the signal from [<sup>13</sup>C]bicarbonate.

## Methods

All animal experiments were approved by the Danish Animal Experiments Inspectorate.

### Animal model of LAD occlusion

The animal model of LAD occlusion was performed in 10 rats in paper I. Anesthesia was maintained with 1.7 - 2% isoflurane in a mixture of air and 5% oxygen. For additional pain relief 0.05 µg/g buprenorphine (Temgesic, Reckitt Benckiser, Denmark) was given s.c. 15-30 minutes before surgery. The rats were intubated and connected to a small animal ventilator (SAR-830/P, IITC Life Science, USA). Respiration was kept at 72 breaths/minute. pCO<sub>2</sub> was monitored on a NPB-75MAX Capnograph (Nellcor Puritan Bennett Inc, USA) connected to the ventilator. Myocardial ischemia was induced by previous described techniques (59, 60). After a left thoracotomy and a pericardiectomy, the LAD was occluded by placing a ligature around the branch. Ischemia was verified visually by bleaching and blue-coloring of the myocardium distal to the occlusion. The ligature was placed in order to achieve an ischemic area covering approximately 1/2 of the anterior wall of the left ventricle including the apex (figure 2). The LAD was occluded for 30 min resulting in a situation of severe ischemia. Ischemia was followed by reperfusion, which was achieved by releasing the tension of the ligature. The rats were scanned with hyperpolarized [1-<sup>13</sup>C]pyruvate before and 2 hours after reperfusion. During scanning the animals were placed on a heating pad and temperature, ECG and expiration gases were monitored (body temperature: 37.0-38.0 °C, expiration CO<sub>2</sub>: 3.5 – 4.0 kPa).

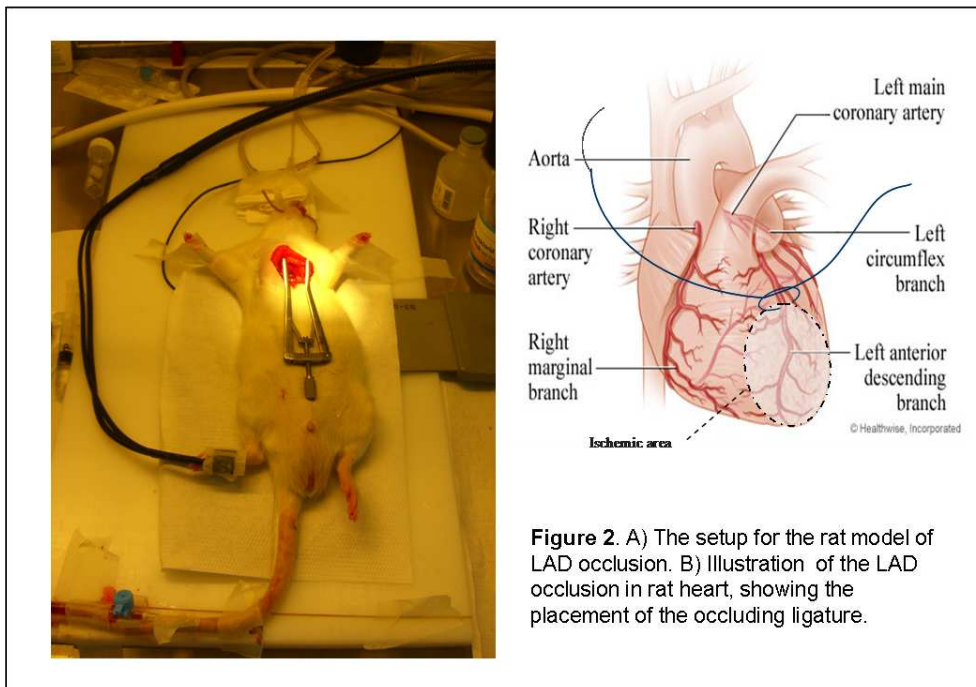


**Figure 2.** A) The setup for the rat model of LAD occlusion. B) Illustration of the LAD occlusion in rat heart, showing the placement of the occluding ligature.

## **GIK infusion**

GIK infusion was performed in paper II. Two tail vein catheters were inserted, one for infusion of GIK and another for administration of hyperpolarized [1-<sup>13</sup>C]pyruvate. The rats were randomly separated into two groups. The first group (n=6) was infused for one hour with a high dose of GIK (25 mg/kg/min glucose, 5 mU/kg/min insulin and 10 mmol/kg/min potassium). The second group (n=5) received a lower dose (15 mg/kg/min glucose, 3 mU/kg/min insulin and 10 mmol/kg/min potassium). The insulin was a fast-acting type (Actrapid, Novo Nordisk A/S, Denmark). The rats were scanned three times with hyperpolarized [1-<sup>13</sup>C]pyruvate. 1: In the fasted state, 2: Immediately after infusion of GIK and 3: One hour post GIK infusion. Prior to each scan blood was collected for blood glucose measurements (see later in this section).

## **[1-<sup>13</sup>C]pyruvate sample preparation**

In both papers 20 uL (~26 mg) of [1-<sup>13</sup>C]pyruvic acid (Sigma Aldrich, Germany) was mixed with 15 mM trityl radical OX063 (Oxford Instruments, UK) and 1.5 mM Dotarem (Guerbet, France) and loaded into a HyperSense polarizer (Oxford Instruments, UK). The sample was dissolved in a neutralizing buffer (80 mM TRIS, 100 mg/L EDTA, 50 mM NaCl, 80 mM NaOH) achieving a final concentration of 80 mM [1-<sup>13</sup>C]pyruvate (pH 7.0-8.0, temperature ~37 °C, isotonic).

## **MR system and hardware**

In preclinical setups the field strength typically ranges from 4.7 T to 9.4 T but much higher field strength (e.g. 21 T) has been developed. In this study a 4.7 T horizontal bore magnet was used for the MR experiments. The magnet was equipped with a Varian Direct Drive console and the Vnmrj 2.3A software was used for acquisition (Agilent Technologies, 5301 Stevens Creek Blvd, Santa Clara CA 95051, US). The rats were placed in a <sup>13</sup>C/<sup>1</sup>H radiofrequency (RF) volume coil, and a <sup>13</sup>C circular receive surface coil or a <sup>13</sup>C four channel array coil (receive-only), with a curved surface, was placed over the heart (both RF coils from RAPID Biomedical GmbH, Germany). The inner diameter of the volume coil was 72 mm. The receive channel array consisted of 4 elements of length 42.5 mm with a sensitivity reaching approximately 20 mm into the animal. The diameter of the surface coil was 20 mm. The surface coil was sensitive to a depth of approximately 15 mm into the animal.

## **Anatomical MRI and late enhancement**

prior to the <sup>13</sup>C MRS scans anatomical long axis proton MR-images were acquired for spatial localization of the heart and for control of correct coil positioning using a ECG and respiratory gated Cine pulse sequence (TR = 195 ms; TE = 3 ms; FOV = 60 x 120 mm<sup>2</sup>; Slice thickness = 2

mm; Matrix size = 128 x 256, Number of cardiac phases = 8). The position of the coils was verified by an external marker (oil pellet) placed on the top and in the centre of the surface coil. On the array coil, the oil pellet was placed on one side of the coil and the animal was placed so the most sensitive part of the coil was closest to the heart. Proton LE images were acquired for visualization of infarct area after the hyperpolarized  $^{13}\text{C}$  MRS sessions, because gadolinium is known to destroy the polarization of the  $^{13}\text{C}$  labelled substrate. ECG-gated inversion recovery gradient echo MR images were obtained 10-20 minutes after the injection of 0.3 mmol/kg gadolinium based contrast agent (Dotarem, Guerbet, USA). The inversion time was adjusted individually for each rat (350-500 ms) to obtain the best contrast between the gadolinium enhanced tissue and the surrounding healthy tissue (TR = 600 ms; TE = 10 ms; FOV = 60 x 120 mm<sup>2</sup>; Slice thickness = 2 mm; Matrix size = 192 x 512).

### **Chemical shift imaging**

An ECG and respiratory-gated slice-selective chemical shift imaging (CSI) sequence was used (Slice thickness = 5 mm, flip angle = 10 °, Circular spiral k-space trajectory matrix with 144 phase encoding steps, TR = 69 ms TE = 1.86 ms, FOV = 25 x 25 mm<sup>2</sup>) The CSI sequence was acquired 7 seconds after end of [1- $^{13}\text{C}$ ]pyruvate injection from the same long axis slice through the heart as the one used for the proton cine imaging.

### **Evaluation of Troponin I and blood glucose levels**

In both papers a catheter was introduced in the left femoral artery for collection of blood. In paper I blood (400 uL) was collected pre-ischemia and 1 and 2 hours after reperfusion (post-ischemia) for evaluation of tissue damage, by the cardiac specific biomarker Troponin I. The level of Troponin I was analyzed on an AQT90 Flex (Radiometer, Denmark), which is an immunoassay technology based on antibodies against Troponin I and fluorescence measurements. In paper II blood (2 uL) was collected from the femoral artery prior to each hyperpolarized  $^{13}\text{C}$  MRS scan. Blood glucose levels were analysed directly on an OneTouch Ultra 2 (LifeScan, Denmark) full blood glucose analyser, which uses the glucose oxidase technology for measuring concentration of glucose.

### **MRS analysis**

A tool for analysis of the acquired MRS-data were implemented in MATLAB (The Mathworks, Natick MA) and applied as described below. In paper I, a two-dimensional CSI sequence was used with a Cartesian circular spiral phase encoding covering a 12 x 12 matrix. The first point in the spiral sequence started at the centre of k-space (low frequencies) determining the signal to noise ratio (SNR) and the last point was acquired in the outer part of the k-space (high frequencies) determining the image resolution. Modulus spectrum analysis was used due to a

relatively large phase-dispersion across the k-space. A combined exponential line-broadening and sine bell line-narrowing filter was used, to separate the metabolic peaks in the modulus spectrum. The signals were then apodized and zero-filled to a matrix size of 32 x 32 along the spatial dimensions. The spectral analysis was performed by integrating the [1-<sup>13</sup>C]lactate, [1-<sup>13</sup>C]alanine and [<sup>13</sup>C]bicarbonate signals at predefined frequency offsets relative to the frequency of the pyruvate peak.

The CSI data were presented as metabolic maps, which were registered to the corresponding first cardiac phase Cine image. The effect of ischemia was quantified by a line profile of the metabolite signal. A line was drawn from the apex along the anterior wall of the myocardium on the cine image, covering both the healthy part (proximal) and the ischemic part (distal) of the myocardium. A typical example of how the line was placed on the first cardiac phase proton cine image is shown in figure 4A and 4B (column 5) as well as on the metabolic maps in figure 4C (column 1-4). The metabolite signal values from the corresponding voxels of the line profile on the metabolite maps were collected and normalized to the maximal signal along the measured line profile (100%). The signals were plotted as the distance from apex (mm) for each animal pre-ischemia and post-ischemia. The distance from where the signal reached 50% of maximum was used for comparison between healthy (pre-ischemia) and diseased (post-ischemia) hearts.

In paper II, dynamic <sup>13</sup>C MR spectra were acquired from a non-gated 5 mm long axis slice every second for 120 min, with a low flip angle of 10°. The spectra from each of the four coil elements was summed from the maximum of the pyruvate bolus peak over a 30 s time window (30 spectra) to effectively generate area-under-the-curve signals. The metabolite signals were quantified using an in house Hankel singular value decomposition (HSVD) method written in MATLAB (61), the individual data from each coil elements was combined retrospectively. The method sums up all signals that are greater than the noise within a priori defined frequency spans.

## Statistics

In paper I, paired two-tailed student t-test was performed to evaluate the difference between group mean values from the line profile evaluation pre and post ischemia, for both [1-<sup>13</sup>C]alanine and [1-<sup>13</sup>C]lactate. Statistical significance was considered at the  $p \leq 0.05$  level. No statistic evaluation was made on the Troponin I data as the sham group only consisted of two values and that is not enough to base a statistical analysis on.

In Paper II, repeated measurement analysis of variance (ANOVA) was performed to evaluate the difference between group mean values of [1-<sup>13</sup>C]alanine/[1-<sup>13</sup>C]pyruvate, [1-<sup>13</sup>C]lactate/[1-<sup>13</sup>C]pyruvate ratios and blood glucose values. Because the [<sup>13</sup>C]bicarbonate signal was below the detection limit in both the fasted and post GIK state (low dose), single sample two-tailed t-test of mean equal to zero, were used to compare differences in the [<sup>13</sup>C]bicarbonate/[1-<sup>13</sup>C]pyruvate ratio between fasted state and GIK and between GIK and post GIK in both the low

and the high dose group. Unpaired two-tailed t-test was used to compare differences in [<sup>13</sup>C]bicarbonate/[1-<sup>13</sup>C]pyruvate ratio between the low and the high dose group. Statistical significance was considered at the  $p \leq 0.05$  level.

## Main Results

The results are presented in two main sections each representing one paper.

### *Paper I.*

#### *Visualizing myocardial ischemia using Hyperpolarized 1-<sup>13</sup>C pyruvate MRS*

##### *Initial optimization*

The advantage of the experimental animal model of LAD occlusion is that it allows for examination of a non ischemic (healthy) part of the heart as well an ischemic (diseased) part of the heart, within the same animal. In this way the animal can be used as it own control. However, optimization of the imaging protocol was made in healthy rats. First we examined if all pyruvate metabolites could be visualized in the non-ischemic heart. This included optimization of [1-<sup>13</sup>C]pyruvate polarization, injection time and rate, optimization of CSI sequence acquisitions, choice of coil, position of the coil, selection of slice placement including slice thickness and ECG triggering.

Initially the non-ischemic hearts were examined using dynamic time series. During injection of 1 mL of 80 mM hyperpolarized [1-<sup>13</sup>C]pyruvate (injection rate 7-8 seconds) signal was detected every second for 120 seconds from a 5 mm slice through the heart. In this way the injected [1-<sup>13</sup>C]pyruvate and the formation of its metabolites in the myocardium could be follow over time. The time series was used to determine the best time period for acquiring the CSI data in order to detect all metabolites. This was important because the CSI sequence was relatively long (30-35 seconds). The reason was primarily that we decided to use an ECG triggered CSI sequence. The acquiring of data was thereby dependent on the heart rate of the rat. We found that the ECG triggered sequence generated more confined metabolic images than the un-triggered sequence (figure 3). It was decided to acquire the CSI data 7 seconds after end of [1-<sup>13</sup>C]pyruvate injection.

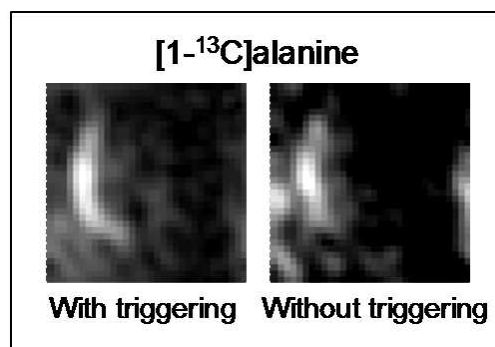


**Figure 3.** Metabolic images of [1-<sup>13</sup>C]alanine comparing the results of a normal CSI sequence with a ECG and respiratory-triggered sequence.

Parallel to the imaging optimization, optimization of the animal surgical procedure was performed. Because the LAD occlusion procedure is very invasive, the initial survival rate was low (only approximately 50%). However, practise made it possible to increase the survival rate to approximately 80%. Some of the most common complications during surgery were bleeding from the mamma artery, puncture of the lungs, puncture of LAD and ventricular fibrillation followed by cardiac arrest. Examples of death due to extensive bleeding from arteria femoralis during the blood sampling procedure, was also observed. An LAD occlusion time of 30 min was chosen as a severe ischemic condition, referring to other similar experiment in the literature and to the high levels of Troponin I measured in the blood after 1 hour of reperfusion. Furthermore, the experience was, that the longer occlusion time the higher was the likelihood for not achieving reperfusion, which was of great importance in this study to ensure that the hyperpolarized  $[1-^{13}\text{C}]$ pyruvate was delivered to ischemic area.

After optimization of the protocol we were able to observe hyperpolarized  $^{13}\text{C}$  signal from  $[1-^{13}\text{C}]$ pyruvate and its metabolites  $[1-^{13}\text{C}]$ lactate,  $[1-^{13}\text{C}]$ alanine and  $[^{13}\text{C}]$ bicarbonate in the healthy non-ischemic rat heart (figure 4). The  $[1-^{13}\text{C}]$ pyruvate signal was confined to the ventricles, whereas  $[1-^{13}\text{C}]$ lactate,  $[1-^{13}\text{C}]$ alanine and  $[^{13}\text{C}]$ bicarbonate signal was confined to the myocardium (figure 4A). Due to limited coil sensitivity signal from  $[1-^{13}\text{C}]$ lactate,  $[1-^{13}\text{C}]$ alanine and  $[^{13}\text{C}]$ bicarbonate was primarily detected in the anterior wall of the myocardium closest to the coil, using a simple surface receive coil. A better coverage was suggested by changing the coil to a four channel array receive coil with a curved surface. However, even though the coverage was slightly improved with the four channel array coil, it was not enough to detect signal from the posterior part of the myocardium, so data from both coils was included in this study. A long axis slice was chosen. In this way signal could be detected from the entire anterior wall, covering both the healthy part (proximal) of the heart and the ischemic part (distal).

In paper I, the myocardial metabolism was compared pre- and post-ischemia in 10 rats. When looking at the metabolic images visually, loss of signal was detected in the  $[1-^{13}\text{C}]$ alanine images in the area corresponding to the ischemic area (figure 4B). LE imaging supported this. Elevated signal in the LE images was observed in the area, which showed reduced  $^{13}\text{C}$  signal in the  $[1-^{13}\text{C}]$ alanine maps (figure 4C, last column).

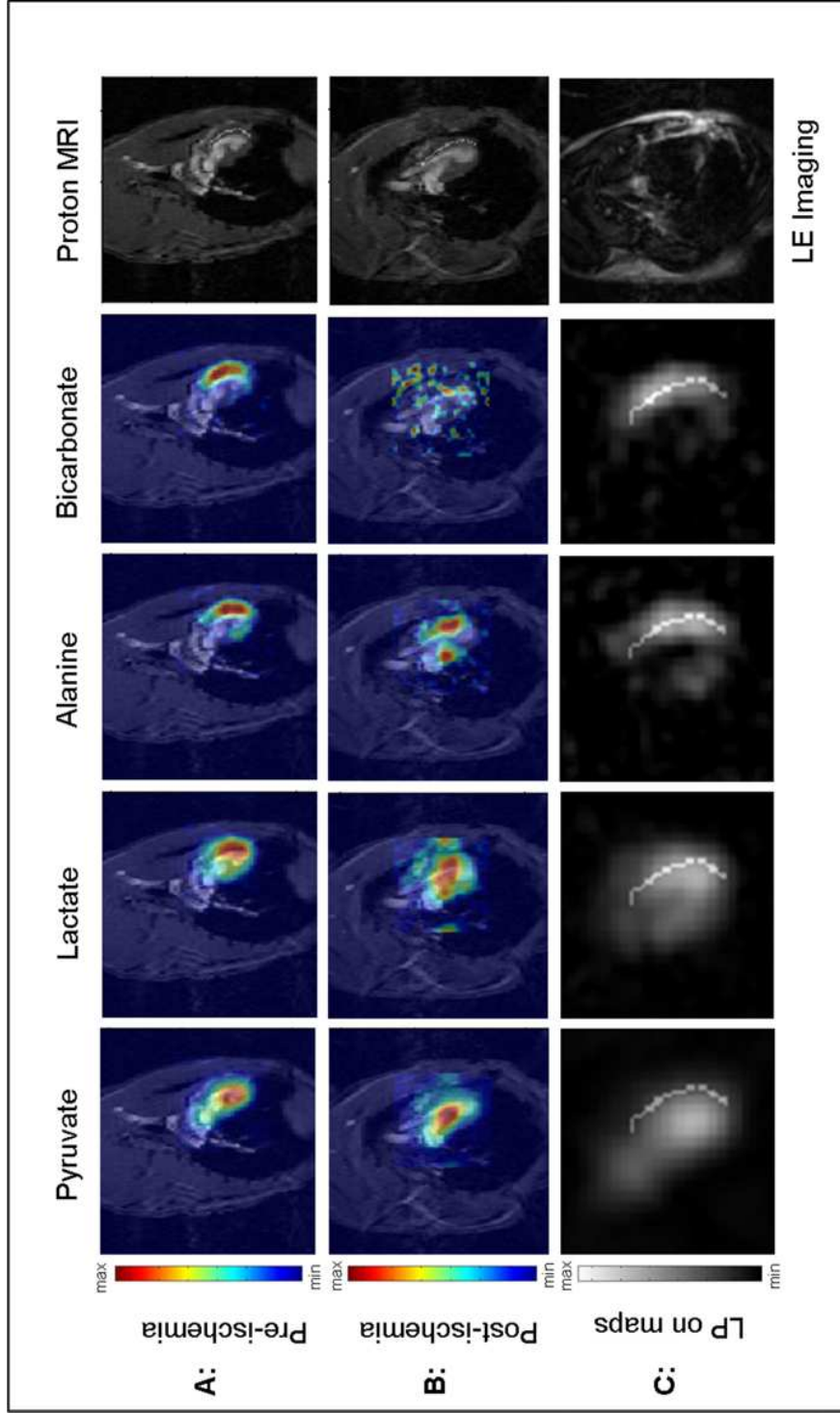


**Figure 4:** Representative metabolic images of cardiac metabolism (A) pre-ischemia (healthy heart) and (B) post-ischemia (30 min ischemia followed by 2 hours reperfusion) for  $[1-^{13}\text{C}]\text{pyruvate}$ ,  $[1-^{13}\text{C}]\text{lactate}$ ,  $[1-^{13}\text{C}]\text{alanine}$  and  $[^{13}\text{C}]\text{bicarbonate}$  respectively (FOV = 25 x 25 mm, slice thickness = 5 mm, FA = 10°). The proton MRI (last column to the right) shows an example of how the line used for the line profile (LP) analysis is drawn on the proton cine-images. (C) Shows the LP as overlay on the metabolic maps pre-ischemia in black and white. The corresponding post-ischemia late enhancement (LE) image is shown down in the right corner. Enhanced signal can be observed in the distal ischemic region of the anterior myocardial wall including in the tissue of the anterior chest wall.

The line profile made it possible to quantify the signals and compare healthy and ischemic hearts. A significant decrease was observed in the  $[1-^{13}\text{C}]$ alanine signal in the distal region of the anterior wall (ischemic region) post-ischemia compared to pre-ischemia (figure 5). The distance for which the  $[1-^{13}\text{C}]$ alanine signal reached 50% of max was  $2.3 \text{ mm} \pm 0.43 \text{ mm}$  (mean  $\pm$ standard error) pre-ischemia and  $6.4 \text{ mm} \pm 1.0 \text{ mm}$  (mean  $\pm$ standard error) post-ischemia with a difference of  $4.1 \text{ mm}$  (CI-95%,  $p = 0.0053$ ) (figure 5A). A smaller difference in mean distance between pre- and post-ischemia was detected in the  $[1-^{13}\text{C}]$ lactate signal level than in the  $[1-^{13}\text{C}]$ alanine signal level (figure 5B). The mean distance for which the  $[1-^{13}\text{C}]$ lactate signal reached 50% of max was  $1.4 \text{ mm} \pm 0.45 \text{ mm}$  (mean  $\pm$ standard error) pre-ischemia and  $3.6 \text{ mm} \pm 0.79 \text{ mm}$  (mean  $\pm$ standard error) post-ischemia with a difference of  $2.2 \text{ mm}$  (CI-95%,  $p = 0.042$ ).

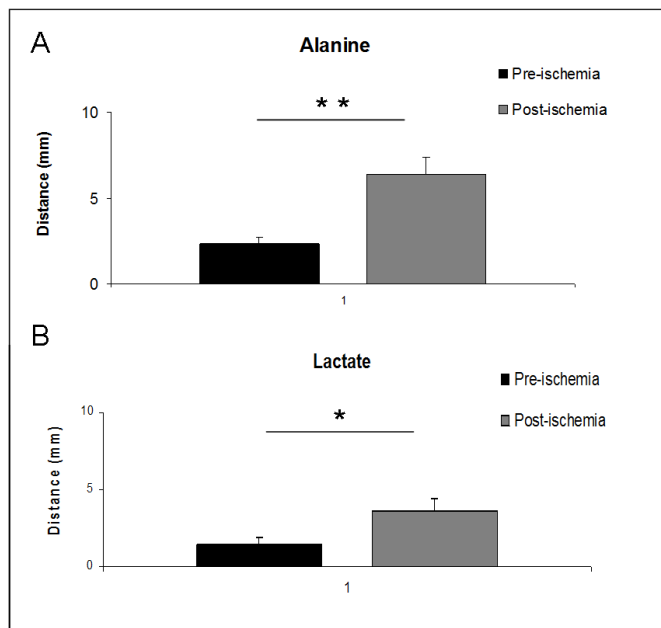


**Figure 5.** Mean distances from the line profile analysis of (A)  $[1-^{13}\text{C}]$ alanine and (B)  $[1-^{13}\text{C}]$ lactate. Line profiles drawn on the anterior wall of the myocardium for  $[1-^{13}\text{C}]$ alanine. The signals were plotted as distance from apex (mm) for each animal (A) pre-ischemia and (B) post-ischemia. The mean distance for which the signal reached 50% is significant longer post-ischemia compared to pre-ischemia for both  $[1-^{13}\text{C}]$ alanine and  $[1-^{13}\text{C}]$ lactate (\*\*  $p < 0.01$ , \*  $p < 0.05$ ).

Due to problems with the blood drawing during scanning Troponin I blood levels were only measured post-ischemia in 6 out of 10 rats. The results are shown in figure 6. In two animals the last sample was taken approximately 3 hours after reperfusion, when the rat was removed from the scanner. The Troponin I level peaked 1 hour after reperfusion and continued to be elevated 2-3 hours after reperfusion. The mean value

of Troponin I one hour after reperfusion was  $41.0 \text{ ng/mL} \pm 13.2 \text{ ng/mL}$  (mean  $\pm$  standard deviation) in the infarcted group and  $0.13 \text{ ng/mL}$  and  $0.93 \text{ ng/mL}$  in the two sham operated rats respectively.

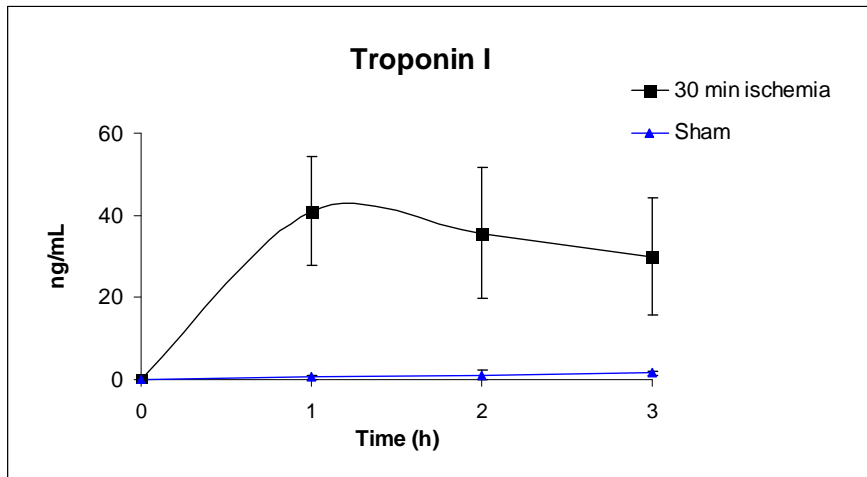


**Figure 6.** Blood levels of Troponin I measured pre-ischemia (0 hours) and 1,2 and 3 hours after reperfusion in ischemic (n = 7) and sham operated rats (n =2). The Troponin I level peaked after 1 hour of reperfusion ( $41.0 \text{ ng/mL} \pm 13.2 \text{ ng/mL}$  (mean  $\pm$  SD) in the ischemic rats.

## Paper II.

### *Enhancing the [ $^{13}\text{C}$ ]bicarbonate signal in cardiac hyperpolarized [ $1\text{-}^{13}\text{C}$ ]pyruvate MRS studies by infusion of glucose, insulin and potassium.*

It is generally very important to have a well controlled preclinical set up to be able to interpret correctly on the results. The experience from the first paper was that the [ $^{13}\text{C}$ ]bicarbonate often was under the detection limit post-ischemia, where the experiment was more time consuming. Due to the surgical procedure, the rats were scanned later during the day compared to the pre-ischemic scanning.

In contrast to the previous paper in paper II the [ $^{13}\text{C}$ ]bicarbonate signal was examined using dynamic time series and not CSI imaging, because we were interested in the total amount of signal and not the spatial information as so. The [ $^{13}\text{C}$ ]bicarbonate signal was measured in relation to the signal from [ $1\text{-}^{13}\text{C}$ ]pyruvate as a [ $^{13}\text{C}$ ]bicarbonate/[ $1\text{-}^{13}\text{C}$ ]pyruvate ratio. Figure 7 shows the results from the GIK study. Two different doses of GIK were examined in fasted rats, a low dose and a high dose. No [ $^{13}\text{C}$ ]bicarbonate could be detected in the fasted state. However after 1 hour infusion of GIK a significant increase in [ $^{13}\text{C}$ ]bicarbonate could be detected in the high dose group ( $p = 0.01$ ) compared to zero (represented as the fasted state). Increase in [ $^{13}\text{C}$ ]bicarbonate was also detected in the low dose group after GIK infusion, but this failed to reach significance ( $p = 0.12$ ). A threefold higher [ $^{13}\text{C}$ ]bicarbonate signal was observed in the high dose group compared to the low dose group with a difference of  $-0.04$  ( $p = 0.03$ ). One hour



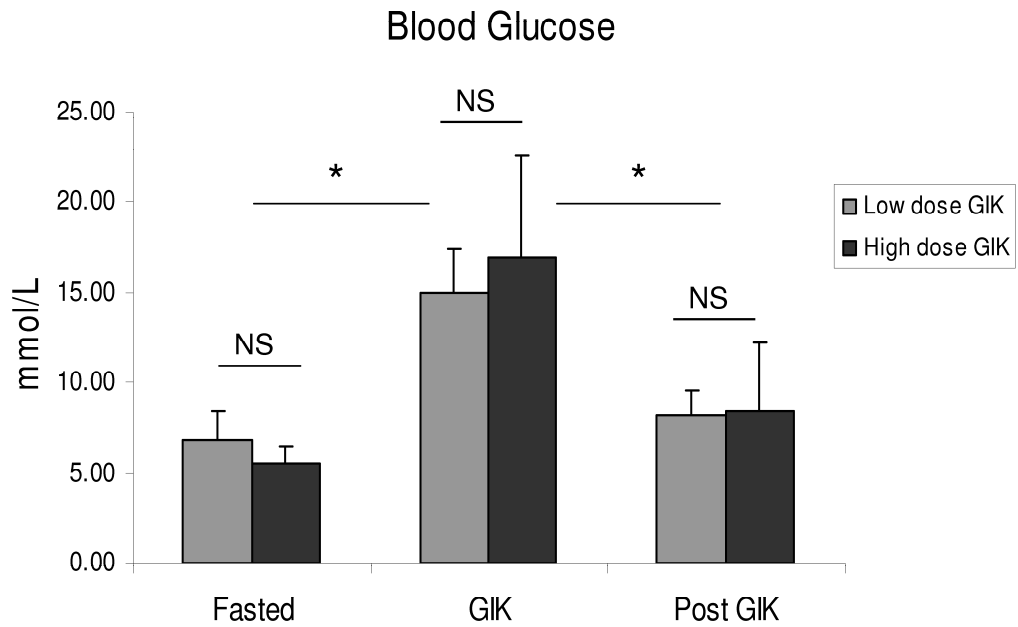


**Figure 8.** Blood glucose levels in rats given a high dose and a low dose of GIK respectively: In the fasted state, after 1 hour of GIK infusion and 1 hour post GIK infusion. Significant increase was observed in the low dose group (\* $p = 0.0003$ ) and the high dose group (\* $p = 0.002$ ) after GIK infusion compared to fasted.

## Discussion

Imaging of myocardial ischemia in rats opposes several challenges. The heart is small and beats very fast (rats: 350-400 bpm). Because of its size, the MR-signals from the  $^{13}\text{C}$  labelled metabolites are low and require suited hardware to detect. Furthermore, occlusion of the LAD in rats has to be done with an open chest surgical procedure, which is quite invasive and can be difficult to perform. However, the ischemic rat model of LAD occlusion is a well validated model, which is used World wide for research in cardiac metabolism, and in more commercial point of views to test the effect of different treatments and for evaluation of new interventions against myocardial ischemia. The blood supply to rat myocardium is similar to the human heart, but with some differences. As in humans the LAD is predominant and supplies the left ventricle. There is no true circumflex artery. In contrast to human coronary arteries, the arteries of rats lies beneath the surface of the heart buried in the myocardium, making it difficult to see and place the LAD occluding ligature during surgery. Another distinguished feature of the rat heart is that the coronary arteries are end-arteries, and that inter-arterial anastomoses are rare. This means that a LAD occlusion in rats may result in more severe ischemia or a larger ischemic area than in humans or pig hearts that have anastomoses, which can supply the ischemic area to some extent. Another important issue to consider is that the rats are anesthetised during the experiment. Anaesthesia is known to affect metabolism. However, Isofluran affect metabolism to a lesser extent than other drugs used for anaesthesia in rats (62). Though, increased plasma glucose has been documented with Isofluran (63, 64). Interestingly, Isofluran has shown to increase the uptake of  $^{18}\text{F}$ FDG in mice myocardium (65). Thus, Isofluran could in theory affect our measurements from the hyperpolarized  $^{13}\text{C}$  MRS studies in paper I, between rats anesthetised for a shorter period (post-ischemia) compared to the ones anesthetised for a longer period (post-ischemia). However, there was no sign of increased glucose uptake or utilization in the rat hearts post-ischemia, rather the opposite, as explained in detail later in this section. Furthermore, the anaesthesia was not believed to affect the results from the hyperpolarized  $^{13}\text{C}$  MRS studies in paper II, where the rats were anesthetised in the same amount of time with approximately the same dose of anaesthesia.

The first part of the thesis was used to establish the surgical ischemic rat model in the laboratory including optimization of blood drawing for Troponin I measurements. Furthermore, the hyperpolarized  $[1-^{13}\text{C}]$ pyruvate MRS protocol in healthy rat hearts was optimized as well as optimization of conventional MRI imaging and LE imaging, which was used to support the hyperpolarized  $[1-^{13}\text{C}]$ pyruvate MRS results. More supportive measurement could have been included in the thesis, but it was limited by lack of time, expertise and facilities to perform e.g. molecular and histological analysis.

After optimization of the hyperpolarized  $^{13}\text{C}$  MRS protocol in healthy rats, we were able to detect signal from  $[1-^{13}\text{C}]$ pyruvate,  $[1-^{13}\text{C}]$ lactate,  $[1-^{13}\text{C}]$ alanine and  $[1-^{13}\text{C}]$ bicarbonate in the rat heart and we were able to construct defined metabolic images of the of the myocardium closest to the coil with good spatial resolution. In the initial studies a simple circular  $^{13}\text{C}$  surface receive coil was used, which had a limited sensitivity. A better coverage of the heart was

attempted by changing the coil to a curved 4 channel array coil. Though a slightly better coverage was achieved with the 4 channel array coil, it was not enough to detect  $^{13}\text{C}$  signal from the posterior part of the myocardium. In paper I the consequences of the limited coil sensitivity was overcome by choosing a longaxis slice that covered the entire anterior wall of the myocardium including both the ischemic and healthy region of the myocardium, which was used for quantification of signal differences between healthy hearts (pre-ischemia) and ischemic hearts (post-ischemia). However, for further optimization a fully coverage of the heart would be preferable.

The results obtained in this thesis and other studies with hyperpolarized  $[1-^{13}\text{C}]$ pyruvate suggest that it is possible, to not only to image and diagnose ischemia, but also determine the severity of tissue damage. As described in the introduction  $[^{13}\text{C}]$ bicarbonate is produced in the mitochondrial membrane and  $[1-^{13}\text{C}]$ lactate and  $[1-^{13}\text{C}]$ alanine is produced in the cytoplasm. In mild situations of ischemia the mitochondrial activity is depressed due to lack of oxygen required for oxidative phosphorylation in the TCA cyclus. This can be observed as a decrease in the  $[^{13}\text{C}]$ bicarbonate signal and an increase in the lactate signal, because the PDH activity is depressed and the LDH activity is enhanced (17). However, even in a situation of depressed mitochondrial activity, the overall cellular metabolism may still be intact and the cells in the ischemic region could still survive, if the blood supply is re-established. But in severe and prolonged situations of ischemia the entire cellular metabolism will be affected and signal from all metabolites, including  $[1-^{13}\text{C}]$ alanine and  $[1-^{13}\text{C}]$ lactate would be decreased (53, 54). This would most likely lead to cell death because the cells can not survive without any metabolism. This information can not be attained by e.g. PET studies using the radioactive glucose analogue,  $[^{18}\text{F}]$ FDG. Here  $[^{18}\text{F}]$ FDG is taken up by metabolic active cells and accumulates in the cell with no additional information of the further fate of  $[^{18}\text{F}]$ FDG inside the cell.

In Paper I we showed regional changes in cardiac metabolism after 30 min of ischemia and 2 hours of reperfusion. The changes were observed in the  $[1-^{13}\text{C}]$ alanine signal and in the  $[1-^{13}\text{C}]$ lactate signal in the ischemic hearts (post-ischemia) compared to healthy hearts (pre-ischemia). The fact that the  $[1-^{13}\text{C}]$ alanine and  $[1-^{13}\text{C}]$ lactate signal were decreased in the ischemic region of the heart, suggest that 30 min occlusion result in a severe myocardial infarction, with an overall depression of the cellular metabolism in the ischemic region as described above. The severity was verified visually by LE imaging and by an increase in Troponin I blood levels 1 hour after reperfusion. Troponin I is a well known cardiac specific biomarker for myocardial tissue damage, which routinely is used for diagnosis of patients with acute myocardial infarction (2). Unfortunately, we experienced some problems with the blood drawing during scanning, due to clotting of the catheter. The length of the catheter was ~1m from the rat tail to the end of the scanner. In order to avoid clotting of the long catheter, it was flushed with saline containing heparin, but since heparin is know to increase circulating FFA blood levels, we tried to keep the flushing of the catheter to a minimum (less than 1mL), which wasn't enough to avoid clotting in some of the experiments. The variation in the Troponin I signal between rats could be due to variation in the infarct size (placement of the ligature) and variation in the cellular injury that takes place between LAD occlusion and blood sampling.

Surprisingly, in paper I we were not able to assess the [ $^{13}\text{C}$ ]bicarbonate signal post-ischemia as expected, because the overall [ $^{13}\text{C}$ ]bicarbonate signal in metabolic images was under the limit of detection. We hypothesized that the lack of [ $^{13}\text{C}$ ]bicarbonate signal could be due to an overall depression of pyruvate flux through the PDH enzyme complex, due to a switch from glucose utilization towards a higher FFA utilization in the heart. It is known that glucose and FFA compete as substrates for energy production in the heart. Especially during fasting the glucose metabolism declines, FFA utilisation goes up and PDH activity decreases (9, 66). The post-ischemic condition could mimic a “fasted” or rather an “un-fed” condition, because the rats has been anesthetised for a long time before scanning. This hypothesis was however not tested, but could easily have been by measuring e.g. the blood FFA and blood glucose levels e.g. just before scanning.

Nevertheless, in paper II we wanted to test, if it was possible to increase the PDH-flux in fasted rats, by infusion of GIK, seen as an increase of [ $^{13}\text{C}$ ]bicarbonate signal in the myocardium. A GIK-infusion was suggested, because GIK have shown to increase the uptake and utilization of glucose in rats as well as in human hearts (66). Furthermore, in PET studies GIK-infusions have shown to improve image quality by increasing the uptake of [ $^{18}\text{F}$ ]FDG (67, 68).

Two doses of GIK were tested a high dose and a lower dose. Significant increase was observed after GIK-infusion in the high dose group compared to fasted, indicating an increased glucose oxidation and increased flux of pyruvate through PDH. The variation in the data was, however, quite large. This variance could maybe have been reduced if we had been more consistent about slice placement, so variance in how much blood, vessels and surrounding tissue that was included in the slice were minimised. However, some biological variance between animals must be expected. Like other enzymes PDH has a maximum flux limitation. It is likely that more than one hour infusion of GIK is required to reach the maximum PDH flux or at least a steady state in fasted rats. The fast inactivation of PDH (decrease in [ $^{13}\text{C}$ ]bicarbonate signal) post GIK-infusion suggests that the regulation of PDH happens on a faster time scale than one hour, and that a constant infusion is required to ensure high PDH flux during the hyperpolarized  $^{13}\text{C}$  MRS measurements. The blood glucose level was found to increase to the same level independent of the infused GIK dose. Not surprisingly, since the insulin dose is the same relative to glucose in the high dose mixture as the low dose mixture, and the blood glucose clearance rate (uptake of glucose from blood into the cells) depends on the insulin dose.

The PDK inhibitor dichloroacetic acid (DCA) is also known to regulate PDH activity, and has recently been used to increase PDH flux in cardiac hyperpolarized  $^{13}\text{C}$  MRS studies (50, 69, 70). However, severe side effects have been reported using DCA in both animals and humans (71, 72). GIK infusions has already been implemented in cardiac [ $^{18}\text{F}$ ]FDG PET imaging in humans and has been extensively studied in patients with acute myocardial ischemia without side effects. Administration of GIK could therefore be considered a more physiological and less disruptive way to enhance the [ $^{13}\text{C}$ ]bicarbonate signal in animals as well as for clinical applications. It should, however, be noted that [ $^{13}\text{C}$ ]bicarbonate signal may be achieved just by ensuring a fully fed condition during the time of scanning, which is possible in most clinical settings.

In relation to ischemia, it could be interesting to test if GIK-infusion affects the PDH-flux the same way in ischemic rat hearts, than in healthy rat hearts. Recently it has been suggested that the hearts ability to shift between substrates for energy metabolism can be reduced in e.g. chronic heart failure, diabetes and other metabolic diseases (73-75). GIK-infusions could potentially be used in future hyperpolarized  $^{13}\text{C}$  MRS studies to evaluate the heart's metabolic "flexibility" or rather in-flexibility, as a marker of disease.

Since it is known that the myocardial glucose metabolism and PDH activity is decreased in diabetic hearts (51), and that GIK routinely is used in diabetic patients to increase the uptake of the glucose analogue [ $^{18}\text{F}$ ]FDG in PET studies (76), it could be interesting to examine how GIK infusion affect cardiac metabolism in diabetic hearts with hyperpolarized [ $1\text{-}^{13}\text{C}$ ]pyruvate MRS compared to e.g. non diabetic hearts. Another interesting study could be to examine the effect of an oral glucose load with GIK-infusion in healthy rats. One could speculate that an oral glucose load were able to increase the [ $^{13}\text{C}$ ]bicarbonate signal more slowly, but maybe in a more stable way over time in response to the natural secretion of insulin in the body.

## Conclusion and perspectives

In conclusion the findings in this thesis demonstrate that we are able to assess changes in myocardial metabolism in rats in vivo using hyperpolarized  $^{13}\text{C}$  MRS. Signal from [ $1\text{-}^{13}\text{C}$ ]pyruvate, [ $1\text{-}^{13}\text{C}$ ]lactate, [ $1\text{-}^{13}\text{C}$ ]alanine and [ $^{13}\text{C}$ ]bicarbonate was detected and visualized in healthy rat hearts with good spatial resolution. After 30 min of ischemia changes in the [ $1\text{-}^{13}\text{C}$ ]lactate and [ $1\text{-}^{13}\text{C}$ ]alanine signal could be observed and quantified regionally in the rat myocardium. GIK infusions was able to modulate the hearts substrate metabolism increasing PDH-flux and increasing the [ $^{13}\text{C}$ ]bicarbonate signal in fasted rats hearts. This is interesting because a high PDH-flux is preferable in many cardiac hyperpolarized [ $1\text{-}^{13}\text{C}$ ]pyruvate MRS studies. Generally hyperpolarized  $^{13}\text{C}$  MRS is predicted great potential to advance basic knowledge and to improve diagnosis of cardiac diseases. However, there is a need to focus on improving  $^{13}\text{C}$  image quality in future studies with hyperpolarized  $^{13}\text{C}$  MRS. This includes better hardware, such as coils with better sensitivity, as well as improved MR-sequences to detect low  $^{13}\text{C}$  signals and improved software to analyse the acquired data. New improved sequences for cardiac  $^{13}\text{C}$  imaging have recently been tested in vivo (55, 57, 77) and ways to increase polarisation and prolong the T1-relaxation is explored (78-80). Additionally, other hyperpolarized substrates may offer alternative ways to study cardiac metabolism or specific chemical pathways affected by disease (48). Application of hyperpolarized  $^{13}\text{C}$  MRS in patients with cardiovascular disease has not been reported yet. However, recently a study of hyperpolarized [ $1\text{-}^{13}\text{C}$ ]pyruvate in patients with prostate cancer was published (81) and two Danish hospitals have recently acquired the technology to perform research studies in humans. However, successful translation of cardiac hyperpolarized  $^{13}\text{C}$  MRS into clinic will require an extensive understanding of the biological systems examined. Regulation of cardiac metabolism is complex and is influenced by several factors especially during disease, which can complicate

the interpretation of the data obtained. Animal models such as the rat LAD occlusion model and other in vivo models may contribute with important knowledge for future hyperpolarized  $^{13}\text{C}$  MRS studies in humans.

## References

1. Guilbert JJ. The world health report 2. Educ Health (Abingdon ) 2003;16(2):230.
2. Tiwari RP, Jain A, Khan Z, Kohli V, Bharmal RN, Kartikeyan S, Bisen PS. Cardiac troponins I and T: molecular markers for early diagnosis, prognosis, and accurate triaging of patients with acute myocardial infarction. *Mol Diagn Ther* 2012;16(6):371-381.
3. Braunwald E. Biomarkers in heart failure. *N Engl J Med* 2008;358(20):2148-2159.
4. Miller CD, Fermann GJ, Lindsell CJ, Mahaffey KW, Peacock WF, Pollack CV, Hollander JE, Diercks DB, Gibler WB, Hoekstra JW. Initial risk stratification and presenting characteristics of patients with evolving myocardial infarctions  
1. *Emerg Med J* 2008;25(8):492-497.
5. Bing RJ, Siegel A, Vitale A, Balboni F, Sparks E, Taeschler M, Klapper M, Edwards S. Metabolic studies on the human heart in vivo. I. Studies on carbohydrate metabolism of the human heart. *Am J Med* 1953;15(3):284-296.
6. Bing RJ, Siegel A, Ungar I, Gilbert M. Metabolism of the human heart. II. Studies on fat, ketone and amino acid metabolism. *Am J Med* 1954;16(4):504-515.
7. Kraegen EW, Sowden JA, Halstead MB, Clark PW, Rodnick KJ, Chisholm DJ, James DE. Glucose transporters and in vivo glucose uptake in skeletal and cardiac muscle: fasting, insulin stimulation and immunoisolation studies of GLUT1 and GLUT4. *Biochem J* 1993;295 ( Pt 1):287-293.
8. Cooper RH, Randle PJ, Denton RM. Regulation of heart muscle pyruvate dehydrogenase kinase. *Biochem J* 1974;143(3):625-641.
9. Patel MS, Korotchkina LG. Regulation of the pyruvate dehydrogenase complex. *Biochem Soc Trans* 2006;34(Pt 2):217-222.
10. Van d, V, Van BM, Glatz JF. Cardiac fatty acid uptake and transport in health and disease. *Cardiovasc Res* 2000;45(2):279-293.
11. Kerbey AL, Randle PJ, Cooper RH, Whitehouse S, Pask HT, Denton RM. Regulation of pyruvate dehydrogenase in rat heart. Mechanism of regulation of proportions of dephosphorylated and phosphorylated enzyme by oxidation of fatty acids and ketone bodies and of effects of diabetes: role of coenzyme A, acetyl-coenzyme A and reduced and oxidized nicotinamide-adenine dinucleotide. *Biochem J* 1976;154(2):327-348.
12. Muniyappa R, Montagnani M, Koh KK, Quon MJ. Cardiovascular actions of insulin. *Endocr Rev* 2007;28(5):463-491.

13. Kaijser L, Berglund B. Myocardial lactate extraction and release at rest and during heavy exercise in healthy men. *Acta Physiol Scand* 1992;144(1):39-45.
14. Stanley WC, Recchia FA, Lopaschuk GD. Myocardial substrate metabolism in the normal and failing heart. *Physiol Rev* 2005;85(3):1093-1129.
15. Liedtke AJ. Alterations of carbohydrate and lipid metabolism in the acutely ischemic heart. *Prog Cardiovasc Dis* 1981;23(5):321-336.
16. Liedtke AJ, Nellis SH, Mjos OD. Effects of reducing fatty acid metabolism on mechanical function in regionally ischemic hearts. *Am J Physiol* 1984;247(3 Pt 2):H387-H394.
17. Schroeder MA, Atherton HJ, Ball DR, Cole MA, Heather LC, Griffin JL, Clarke K, Radda GK, Tyler DJ. Real-time assessment of Krebs cycle metabolism using hyperpolarized <sup>13</sup>C magnetic resonance spectroscopy. *FASEB J* 2009;23(8):2529-2538.
18. Kurien VA, Oliver MF. Serum-free-fatty-acids after acute myocardial infarction and cerebral vascular occlusion. *Lancet* 1966;2(7455):122-127.
19. Oliver MF, Kurien VA, Greenwood TW. Relation between serum-free-fatty acids and arrhythmias and death after acute myocardial infarction. *Lancet* 1968;1(7545):710-714.
20. Opie LH. Metabolism of free fatty acids, glucose and catecholamines in acute myocardial infarction. Relation to myocardial ischemia and infarct size. *Am J Cardiol* 1975;36(7):938-953.
21. Bax JJ, Visser FC, Poldermans D, Van LA, Elhendy A, Boersma E, Visser CA. Feasibility, safety and image quality of cardiac FDG studies during hyperinsulinaemic-euglycaemic clamping. *Eur J Nucl Med Mol Imaging* 2002;29(4):452-457.
22. Knuuti MJ, Nuutila P, Ruotsalainen U, Saraste M, Harkonen R, Ahonen A, Teras M, Haaparanta M, Wegelius U, Haapanen A, . Euglycemic hyperinsulinemic clamp and oral glucose load in stimulating myocardial glucose utilization during positron emission tomography. *J Nucl Med* 1992;33(7):1255-1262.
23. Gropler RJ, Siegel BA, Lee KJ, Moerlein SM, Perry DJ, Bergmann SR, Geltman EM. Nonuniformity in myocardial accumulation of fluorine-18-fluorodeoxyglucose in normal fasted humans. *J Nucl Med* 1990;31(11):1749-1756.
24. Martin WH, Jones RC, Delbeke D, Sandler MP. A simplified intravenous glucose loading protocol for fluorine-18 fluorodeoxyglucose cardiac single-photon emission tomography. *Eur J Nucl Med* 1997;24(10):1291-1297.

25. Schipke JD, Friebe R, Gams E. Forty years of glucose-insulin-potassium (GIK) in cardiac surgery: a review of randomized, controlled trials. *Eur J Cardiothorac Surg* 2006;29(4):479-485.
26. Whitehouse S, Cooper RH, Randle PJ. Mechanism of activation of pyruvate dehydrogenase by dichloroacetate and other halogenated carboxylic acids  
1. *Biochem J* 1974;141(3):761-774.
27. McVeigh JJ, Lopaschuk GD. Dichloroacetate stimulation of glucose oxidation improves recovery of ischemic rat hearts. *Am J Physiol* 1990;259(4 Pt 2):H1079-H1085.
28. Simpson NE, Han Z, Berendzen KM, Sweeney CA, Oca-Cossio JA, Constantinidis I, Stacpoole PW. Magnetic resonance spectroscopic investigation of mitochondrial fuel metabolism and energetics in cultured human fibroblasts: effects of pyruvate dehydrogenase complex deficiency and dichloroacetate  
2. *Mol Genet Metab* 2006;89(1-2):97-105.
29. Jaswal JS, Keung W, Wang W, Ussher JR, Lopaschuk GD. Targeting fatty acid and carbohydrate oxidation--a novel therapeutic intervention in the ischemic and failing heart. *Biochim Biophys Acta* 2011;1813(7):1333-1350.
30. Wolff AA, Rotmensch HH, Stanley WC, Ferrari R. Metabolic approaches to the treatment of ischemic heart disease: the clinicians' perspective. *Heart Fail Rev* 2002;7(2):187-203.
31. Brown, Semelka. *MRI*. Mosby 2003;3. ed.
32. Bushong. *Magnetic resonance imaging*. Mosby 2003;3. ed.
33. Ishida M, Kato S, Sakuma H. Cardiac MRI in ischemic heart disease. *Circ J* 2009;73(9):1577-1588.
34. Semelka RC, Tomei E, Wagner S, Mayo J, Kondo C, Suzuki J, Caputo GR, Higgins CB. Normal left ventricular dimensions and function: interstudy reproducibility of measurements with cine MR imaging. *Radiology* 1990;174(3 Pt 1):763-768.
35. Oshinski JN, Yang Z, Jones JR, Mata JF, French BA. Imaging time after Gd-DTPA injection is critical in using delayed enhancement to determine infarct size accurately with magnetic resonance imaging. *Circulation* 2001;104(23):2838-2842.
36. Dendale P, Franken PR, Block P, Pratikakis Y, De RA. Contrast enhanced and functional magnetic resonance imaging for the detection of viable myocardium after infarction. *Am Heart J* 1998;135(5 Pt 1):875-880.
37. Dendale P, Franken PR, Meusel M, van der GR, De RA. Distinction between open and occluded infarct-related arteries using contrast-enhanced magnetic resonance imaging. *Am J Cardiol* 1997;80(3):334-336.

38. Garcia-Dorado D, Oliveras J, Gili J, Sanz E, Perez-Villa F, Barrabes J, Carreras MJ, Solares J, Soler-Soler J. Analysis of myocardial oedema by magnetic resonance imaging early after coronary artery occlusion with or without reperfusion. *Cardiovasc Res* 1993;27(8):1462-1469.
39. Holloway CJ, Suttie J, Dass S, Neubauer S. Clinical cardiac magnetic resonance spectroscopy. *Prog Cardiovasc Dis* 2011;54(3):320-327.
40. Schneider JE, Tyler DJ, ten HM, Sang AE, Cassidy PJ, Fischer A, Wallis J, Sebag-Montefiore LM, Watkins H, Isbrandt D, Clarke K, Neubauer S. In vivo cardiac <sup>1</sup>H-MRS in the mouse. *Magn Reson Med* 2004;52(5):1029-1035.
41. Harris DN, Wilson JA, Taylor-Robinson SD, Taylor KM. Magnetic resonance spectroscopy of high-energy phosphates and lactate immediately after coronary artery bypass surgery. *Perfusion* 1998;13(5):328-333.
42. Reingold JS, McGavock JM, Kaka S, Tillery T, Victor RG, Szczepaniak LS. Determination of triglyceride in the human myocardium by magnetic resonance spectroscopy: reproducibility and sensitivity of the method. *Am J Physiol Endocrinol Metab* 2005;289(5):E935-E939.
43. Hudsmith LE, Neubauer S. Magnetic resonance spectroscopy in myocardial disease. *JACC Cardiovasc Imaging* 2009;2(1):87-96.
44. Tyler DJ, Hudsmith LE, Clarke K, Neubauer S, Robson MD. A comparison of cardiac (31)P MRS at 1.5 and 3 T. *NMR Biomed* 2008;21(8):793-798.
45. Brown TR. Practical applications of chemical shift imaging. *NMR Biomed* 1992;5(5):238-243.
46. Brown TR, Kincaid BM, Ugurbil K. NMR chemical shift imaging in three dimensions. *Proc Natl Acad Sci U S A* 1982;79(11):3523-3526.
47. Ardenkjaer-Larsen JH, Fridlund B, Gram A, Hansson G, Hansson L, Lerche MH, Servin R, Thaning M, Golman K. Increase in signal-to-noise ratio of > 10,000 times in liquid-state NMR. *Proc Natl Acad Sci U S A* 2003;100(18):10158-10163.
48. Hurd RE, Yen YF, Chen A, Ardenkjaer-Larsen JH. Hyperpolarized <sup>13</sup>C metabolic imaging using dissolution dynamic nuclear polarization. *J Magn Reson Imaging* 2012;36(6):1314-1328.
49. Merritt ME, Harrison C, Storey C, Jeffrey FM, Sherry AD, Malloy CR. Hyperpolarized <sup>13</sup>C allows a direct measure of flux through a single enzyme-catalyzed step by NMR. *Proc Natl Acad Sci U S A* 2007;104(50):19773-19777.

50. Atherton HJ, Schroeder MA, Dodd MS, Heather LC, Carter EE, Cochlin LE, Nagel S, Sibson NR, Radda GK, Clarke K, Tyler DJ. Validation of the in vivo assessment of pyruvate dehydrogenase activity using hyperpolarised <sup>13</sup>C MRS. *NMR Biomed* 2011;24(2):201-208.
51. Schroeder MA, Cochlin LE, Heather LC, Clarke K, Radda GK, Tyler DJ. In vivo assessment of pyruvate dehydrogenase flux in the heart using hyperpolarized carbon-13 magnetic resonance. *Proc Natl Acad Sci U S A* 2008;105(33):12051-12056.
52. Merritt ME, Harrison C, Storey C, Jeffrey FM, Sherry AD, Malloy CR. Hyperpolarized <sup>13</sup>C allows a direct measure of flux through a single enzyme-catalyzed step by NMR. *Proc Natl Acad Sci U S A* 2007;104(50):19773-19777.
53. Golman K, Petersson JS, Magnusson P, Johansson E, Akeson P, Chai CM, Hansson G, Mansson S. Cardiac metabolism measured noninvasively by hyperpolarized <sup>13</sup>C MRI. *Magn Reson Med* 2008;59(5):1005-1013.
54. Ball DR, Cruickshank R, Carr CA, Stuckey DJ, Lee P, Clarke K, Tyler DJ. Metabolic imaging of acute and chronic infarction in the perfused rat heart using hyperpolarised [<sup>1-13</sup>C]pyruvate. *NMR Biomed* 2013.
55. Lau AZ, Chen AP, Ghugre NR, Ramanan V, Lam WW, Connelly KA, Wright GA, Cunningham CH. Rapid multislice imaging of hyperpolarized <sup>13</sup>C pyruvate and bicarbonate in the heart. *Magn Reson Med* 2010;64(5):1323-1331.
56. Schroeder MA, Clarke K, Neubauer S, Tyler DJ. Hyperpolarized magnetic resonance: a novel technique for the in vivo assessment of cardiovascular disease. *Circulation* 2011;124(14):1580-1594.
57. Lau AZ, Chen AP, Barry J, Graham JJ, Dominguez-Viqueira W, Ghugre NR, Wright GA, Cunningham CH. Reproducibility study for free-breathing measurements of pyruvate metabolism using hyperpolarized (<sup>13</sup>C) in the heart. *Magn Reson Med* 2013;69(4):1063-1071.
58. Moreno KX, Sabelhaus SM, Merritt ME, Sherry AD, Malloy CR. Competition of pyruvate with physiological substrates for oxidation by the heart: implications for studies with hyperpolarized [<sup>1-13</sup>C]pyruvate. *Am J Physiol Heart Circ Physiol* 2010;298(5):H1556-H1564.
59. Johns TN, Olson BJ. Experimental myocardial infarction. I. A method of coronary occlusion in small animals. *Ann Surg* 1954;140(5):675-682.
60. Ye J, Yang L, Sethi R, Copps J, Ramjiawan B, Summers R, Deslauriers R. A new technique of coronary artery ligation: experimental myocardial infarction in rats in vivo with reduced mortality. *Mol Cell Biochem* 1997;176(1-2):227-233.

61. Vanhuffel S. Enhanced Resolution Based on Minimum-Variance Estimation and Exponential Data Modeling. *Signal Processing* 1993;33(3):333-355.
62. Zuurbier CJ, Keijzers PJ, Koeman A, Van Wezel HB, Hollmann MW. Anesthesia's effects on plasma glucose and insulin and cardiac hexokinase at similar hemodynamics and without major surgical stress in fed rats. *Anesth Analg* 2008;106(1):135-42, table.
63. Lattermann R, Schricker T, Wachter U, Georgieff M, Goertz A. Understanding the mechanisms by which isoflurane modifies the hyperglycemic response to surgery. *Anesth Analg* 2001;93(1):121-127.
64. Arnold M, Langhans W. Effects of anesthesia and blood sampling techniques on plasma metabolites and corticosterone in the rat. *Physiol Behav* 2010;99(5):592-598.
65. Fueger BJ, Czernin J, Hildebrandt I, Tran C, Halpern BS, Stout D, Phelps ME, Weber WA. Impact of animal handling on the results of 18F-FDG PET studies in mice. *J Nucl Med* 2006;47(6):999-1006.
66. Kones RJ, Phillips JH. Glucose-insulin-potassium (GIK) therapy for ischemic heart disease. *Crit Care Med* 1975;3(4):143-154.
67. Martin WH, Jones RC, Delbeke D, Sandler MP. A simplified intravenous glucose loading protocol for fluorine-18 fluorodeoxyglucose cardiac single-photon emission tomography. *Eur J Nucl Med* 1997;24(10):1291-1297.
68. Bax JJ, Visser FC, Poldermans D, Van LA, Elhendy A, Boersma E, Visser CA. Feasibility, safety and image quality of cardiac FDG studies during hyperinsulinaemic-euglycaemic clamping. *Eur J Nucl Med Mol Imaging* 2002;29(4):452-457.
69. Atherton HJ, Dodd MS, Heather LC, Schroeder MA, Griffin JL, Radda GK, Clarke K, Tyler DJ. Role of pyruvate dehydrogenase inhibition in the development of hypertrophy in the hyperthyroid rat heart: a combined magnetic resonance imaging and hyperpolarized magnetic resonance spectroscopy study. *Circulation* 2011;123(22):2552-2561.
70. Mayer D, Yen YF, Josan S, Park JM, Pfefferbaum A, Hurd RE, Spielman DM. Application of hyperpolarized [1-(13) C]lactate for the in vivo investigation of cardiac metabolism. *NMR Biomed* 2012.
71. Stacpoole PW. The dichloroacetate dilemma: environmental hazard versus therapeutic goldmine--both or neither? *Environ Health Perspect* 2011;119(2):155-158.
72. Stacpoole PW, Henderson GN, Yan Z, Cornett R, James MO. Pharmacokinetics, metabolism and toxicology of dichloroacetate. *Drug Metab Rev* 1998;30(3):499-539.

73. Taegtmeyer H, Golfman L, Sharma S, Razeghi P, Van AM. Linking gene expression to function: metabolic flexibility in the normal and diseased heart. *Ann N Y Acad Sci* 2004;1015:202-213.
74. Larsen TS, Aasum E. Metabolic (in)flexibility of the diabetic heart  
1. *Cardiovasc Drugs Ther* 2008;22(2):91-95.
75. Neglia D, De CA, Marraccini P, Natali A, Ciardetti M, Vecoli C, Gastaldelli A, Ciociaro D, Pellegrini P, Testa R, Menichetti L, L'abbate A, Stanley WC, Recchia FA. Impaired myocardial metabolic reserve and substrate selection flexibility during stress in patients with idiopathic dilated cardiomyopathy. *Am J Physiol Heart Circ Physiol* 2007;293(6):H3270-H3278.
76. Vitale GD, deKemp RA, Ruddy TD, Williams K, Beanlands RS. Myocardial glucose utilization and optimization of (18)F-FDG PET imaging in patients with non-insulin-dependent diabetes mellitus, coronary artery disease, and left ventricular dysfunction. *J Nucl Med* 2001;42(12):1730-1736.
77. Lau AZ, Chen AP, Cunningham CH. Integrated Bloch-Siegert B(1) mapping and multislice imaging of hyperpolarized (1)(3)C pyruvate and bicarbonate in the heart. *Magn Reson Med* 2012;67(1):62-71.
78. Laustsen C, Pileio G, Tayler MC, Brown LJ, Brown RC, Levitt MH, Ardenkjaer-Larsen JH. Hyperpolarized singlet NMR on a small animal imaging system. *Magn Reson Med* 2012;68(4):1262-1265.
79. Laustsen C, Bowen S, Sloth VM, Chr NN, Ardenkjaer-Larsen JH. Storage of magnetization as singlet order by optimal control designed pulses. *Magn Reson Med* 2013.
80. Marco-Rius I, Tayler MC, Kettunen MI, Larkin TJ, Timm KN, Serrao EM, Rodrigues TB, Pileio G, Ardenkjaer-Larsen JH, Levitt MH, Brindle KM. Hyperpolarized singlet lifetimes of pyruvate in human blood and in the mouse. *NMR Biomed* 2013;26(12):1696-1704.
81. Nelson SJ, Kurhanewicz J, Vigneron DB, Larson PE, Harzstark AL, Ferrone M, van CM, Chang JW, Bok R, Park I, Reed G, Carvajal L, Small EJ, Munster P, Weinberg VK, Ardenkjaer-Larsen JH, Chen AP, Hurd RE, Odegardstuen LI, Robb FJ, Tropp J, Murray JA. Metabolic imaging of patients with prostate cancer using hyperpolarized [1-(1)(3)C]pyruvate. *Sci Transl Med* 2013;5(198):198ra108.

# PAPER I

# Imaging regional metabolic changes in the ischemic rat heart in vivo using hyperpolarized [1-<sup>13</sup>C]Pyruvate

Mette Hauge Lauritzen<sup>1</sup>, Peter Magnusson<sup>1</sup>, Christoffer Laustsen<sup>1,2</sup>, Olaf B. Paulson<sup>1,3</sup>, Sadia Asghar Butt<sup>1</sup>, Jan Henrik Ardenkjær-Larsen<sup>1,4,5</sup>, Lise Vejby Søgaard<sup>1</sup>, Per Åkeson<sup>1</sup>

<sup>1</sup> Danish Research Centre for Magnetic Resonance, Centre for Functional and Diagnostic Imaging and Research, Copenhagen University Hospital Hvidovre, Denmark, <sup>2</sup> MR Research Centre, Institute of Clinical Medicine, Aarhus University Hospital, Aarhus, Denmark, <sup>3</sup> Neurobiology Research Unit, Rigshospitalet, Copenhagen University Hospital Denmark, <sup>4</sup> GE Healthcare, Brøndby, Denmark, <sup>5</sup> Technical University of Denmark, Department of Electrical Engineering, Kgs. Lyngby, Denmark

---

## Abstract

**Background** - Hyperpolarized magnetic resonance spectroscopy (MRS) using <sup>13</sup>C-labeled pyruvate is a non invasive imaging technique, which can detect changes in metabolism in real time following myocardial ischemia. The aim of this study was for the first time to evaluate the use of hyperpolarized [1-<sup>13</sup>C]pyruvate MRS to visualize regional changes in myocardial metabolism in an in vivo rat model of severe ischemia.

**Methods and Results** – 10 rats were examined before and 2 hours after 30 minutes of occlusion of the left anterior descending coronary artery using hyperpolarized [1-<sup>13</sup>C]pyruvate MRS. Cardiac metabolic images of [1-<sup>13</sup>C]pyruvate and its metabolites [1-<sup>13</sup>C]lactate, [1-<sup>13</sup>C]alanine and [<sup>13</sup>C]bicarbonate were obtained pre- and post ischemia. Significant reduction in the [1-<sup>13</sup>C]alanine and [1-<sup>13</sup>C]lactate signals were observed in ischemic heart tissue post-ischemia compared to pre-ischemia. The severity of the ischemic insult was verified by magnetic resonance imaging, showing late contrast enhanced signal in the ischemic region of 7 rats. In 6 rats severe ischemia was also verified by increased blood levels of Troponin I.

**Conclusions** - This study suggest that hyperpolarized [1-<sup>13</sup>C]pyruvate MRS can be used in vivo to visualize regional metabolic changes following myocardial ischemia in the a rat heart. The decrease in the [1-<sup>13</sup>C]alanine and [1-<sup>13</sup>C]lactate signals indicates that the ischemic insult is severe, representing an overall depression of cellular metabolism. This is supported by late enhancement magnetic resonance imaging and increase in Troponin I blood levels. Thus, this study points to a new approach for studies of cardiac metabolism in the in vivo rat heart.

---

## Funding Sources

The authors would like to thank Sascha Gude for her skilful technical assistance and her help with the animals and Marianne Rasmussen for help with the illustrations. This project is supported by grants from The Spies Foundation, The Lundbeck Foundation, The Danish Heart Association and Copenhagen University Hospital Hvidovre.

## Corresponding author

Mette Hauge Lauritzen, e-mail: [metteh@drctr.dk](mailto:metteh@drctr.dk), Phone: +45 62382976, Fax no: +45 36470302, Danish Research Centre for Magnetic Resonance, Centre for Functional and Diagnostic Imaging and Research, Copenhagen University Hospital Hvidovre, Kettegårds Allé 30, 2650 Hvidovre, Denmark

## Disclosures

The authors have no conflict of interest to declare

## Introduction

Myocardial infarction is one of the leading causes of death in the Western countries. Early in the development of the disease, changes in the myocardial metabolism can be observed (1). These changes could potentially be used as diagnostic markers, but have turned out to be difficult to assess non-invasively. Furthermore understanding the functional impact of these changes may be important when developing new metabolic interventions for ischemic heart disease. Conventional magnetic resonance spectroscopy (MRS) of the  $^1\text{H}$ ,  $^{13}\text{C}$ ,  $^{23}\text{Na}$  and  $^{31}\text{P}$  nuclei has previously been used to study cardiac metabolism (2-6), but have primarily been used as research tools due to poor sensitivity. Hyperpolarized MRS using  $^{13}\text{C}$  labeled metabolites is a technique, which can be used to generate metabolic images of the heart and non-invasively visualize changes in metabolism in real time (7). The advantage of hyperpolarized MRS, in contrast to conventional MRS is that it can increase the MRS-signal from the  $^{13}\text{C}$ -labeled metabolites >10.000-fold making it possible to detect low concentrations of the  $^{13}\text{C}$ -labeled metabolites in vivo (8). Hyperpolarized MRS enables monitoring of several steps in metabolic pathways, adding information of the specific enzymatic activities and can in contrast to other existing metabolic imaging techniques, such as positron emission tomography (PET) and single photon emission computed tomography (SPECT), distinguish between the injected compound and its downstream metabolites. It does not expose patients to ionizing radiation and can easily be used in combination with conventional magnetic resonance imaging (MRI) to assess cardiac anatomy, function and mass as well as perfusion and viability with gadolinium-based contrast agents.

The metabolic consequences of myocardial ischemia include increased glycogen breakdown and increased glucose uptake followed by increasing anaerobic glycolysis, increased lactate production and decreased Krebs Cycle (TCA cycle) activity due to the decreasing oxygen availability (1, 9). Pyruvate is the end-

product of the glycolysis and a key substrate for energy production through the TCA cycle. After iv. injection hyperpolarized  $[1-^{13}\text{C}]$ pyruvate is taken up by the myocytes and converted into  $[1-^{13}\text{C}]$ lactate via the enzyme lactate dehydrogenase (LDH) and  $[1-^{13}\text{C}]$ alanine via alanine aminotransferase (ALT), both enzymes located in the cytosol. Furthermore,  $[1-^{13}\text{C}]$ pyruvate is converted into Acetyl CoA via the pyruvate dehydrogenase (PDH) enzyme complex in the mitochondrial membrane and in the process the  $^{13}\text{C}$ -atom in the C-1 position of the pyruvate molecule is transferred to  $^{13}\text{CO}_2$  in equilibrium with bicarbonate via the enzyme carbonic anhydrase (CA) (7, 10, 11). However, often only  $[^{13}\text{C}]$ bicarbonate and not  $^{13}\text{CO}_2$  can be detected with hyperpolarized MRS in vivo, due to sensitivity, since the equilibrium at physiological pH is highly shifted towards bicarbonate. The production of  $[^{13}\text{C}]$ bicarbonate reflects the mitochondrial status, whereas production of  $[1-^{13}\text{C}]$ lactate and  $[1-^{13}\text{C}]$ alanine reflect the general metabolic state of the myocytes, according to the location of the enzymes in the cell (figure 1). Application of hyperpolarized MRS for evaluation of myocardial ischemia has been demonstrated in animals recently (7, 12-15), but generation of metabolic images have not been demonstrated in rats with myocardial ischemia in vivo before. Experiments performed in isolated rat hearts have shown that hyperpolarized  $[1-^{13}\text{C}]$ pyruvate MRS can detect the metabolic consequences of ischemia. Thus, in the study by Schroeder et al. (7) decreased  $[^{13}\text{C}]$ bicarbonate signal and increased  $[1-^{13}\text{C}]$ lactate signal were detected after 10 minutes of global myocardial ischemia, indicating a decreased PDH-flux and increased anaerobic lactate formation via the LDH enzyme. Hyperpolarized  $[1-^{13}\text{C}]$ pyruvate MRS has also been used to generate metabolic images in pigs with myocardial ischemia (13). In this study the left anterior descending coronary artery (LAD) was occluded for 15 minutes (mild ischemia) or 45 minutes (severe ischemia) respectively, followed by 2 hours of reperfusion. Metabolic maps of the  $[1-^{13}\text{C}]$ pyruvate metabolites showed decreased PDH-mediated  $[^{13}\text{C}]$ bicarbonate production after 15 minutes occlusion in the ischemic region of the myocardium. After 45 minutes occlusion both

production of [ $^{13}\text{C}$ ]bicarbonate and [ $^{13}\text{C}$ ]alanine was decreased in the ischemic region representing a depression of both the mitochondrial activity and the overall cellular activity. The metabolic images were compared with gadolinium-based late enhancement (LE) images, which showed enhanced signal after 45 min occlusion but no changes after 15 min occlusion. Thus, this study demonstrates how hyperpolarized  $^{13}\text{C}$  MRS can detect and visualize metabolic changes even during mild ischemic conditions in the heart, before other MR methods such as LE imaging reveals any abnormalities. Application in patients with cardiovascular disease has not been reported yet. However, recently a study of hyperpolarized [ $^{13}\text{C}$ ]pyruvate in patients with prostate cancer was published (16).

The aim of the present study was to investigate if hyperpolarized [ $^{13}\text{C}$ ]pyruvate MRS could be used to visualize regional changes in the myocardial metabolism in an in vivo rat model of severe ischemia. The combination of the hyperpolarized  $^{13}\text{C}$  MRS technique and the in vivo rat model may provide new important information of the disease, and could be used for evaluation of new treatments and metabolic interventions for myocardial ischemia as well as provide knowledge to the potential application in human.

## Materials and Methods

### *Animals, anaesthesia and general procedures*

All experiments were approved by the Danish Animal Experiments Inspectorate.

A total of 12 male Sprague Dawley rats (Taconic Europe, Denmark) weighing 250-350g were examined in this study. 10 animals were examined with hyperpolarized [ $^{13}\text{C}$ ]pyruvate MRS before and 2 hours after ischemia. The remaining two rats were sham operated and used only for evaluation of Troponin I blood levels. All rats were given water and standard rat chow ad libitum. The rats were anesthetized with 5% isoflurane. Anesthesia was maintained with 1.7 - 2% isoflurane in a mixture of air and 5% oxygen. For additional pain relief 0.05  $\mu\text{g/g}$  buprenorphine (Temgesic, Reckitt Benckiser, Søborg, Denmark) was given s.c. 15-30 minutes before surgery. The rats were intubated and

connected to a small animal ventilator (SAR-830/P, IITC Life Science, USA). Respiration was kept at 72 breaths/minute.  $\text{pCO}_2$  was monitored on a NPB-75MAX Capnograph (Nellcor Puritan Bennett Inc, USA) connected to the ventilator. A catheter was introduced into the tail vein for i.v. administration of the hyperpolarized [ $^{13}\text{C}$ ]pyruvate solution. Another catheter was introduced in the left femoral artery for collection of blood. During scanning the animals were placed on a heating pad and temperature, electrocardiogram (ECG), and expiration gases were monitored (body temperature: 37.0-38.0  $^{\circ}\text{C}$ , expiration  $\text{CO}_2$ : 3.5 – 4.0 kPa).

### *Ischemic heart model*

Myocardial ischemia was induced by previous described techniques (17, 18). After a left thoracotomy and a pericardiectomy, the LAD was occluded by placing a ligature around the branch. Ischemia was verified visually by bleaching and blue-coloring of the myocardium distal to the occlusion. The ligature was placed in order to achieve an ischemic area covering approximately 1/2 of the anterior wall of the left ventricle including the apex. The LAD was occluded for 30 min resulting in a situation of severe ischemia. Ischemia was followed by reperfusion, which was achieved by releasing the tension of the ligature. Blood samples were drawn pre-ischemia and 1 and 2 hours after reperfusion for evaluation of tissue damage, by the cardiac specific biomarker Troponin I. The level of Troponin I was analyzed on an AQT90 Flex (Radiometer, Denmark). Two animals were sham operated. In the sham operated animals the surgical procedure was induced as described above, by placing the ligature, but without occluding the artery. The sham operated rats were not scanned, but were used to compare levels of Troponin I.

### *Hyperpolarization*

20  $\mu\text{L}$  (~26 mg) of [ $^{13}\text{C}$ ]pyruvic acid (Sigma Aldrich, Germany) with 15 mM trityl radical OX063 (Oxford Instruments, UK) and 1.5 mM Dotarem (Guerbet, France) was loaded into a polarizer (HyperSense, Oxford Instruments, UK). The sample was dissolved in a neutralizing buffer (80 mM TRIS, 100 mg/L EDTA, 50 mM NaCl, 80 mM NaOH) achieving

a final concentration of 80 mM [ $1\text{-}^{13}\text{C}$ ]pyruvate (pH 7.0-8.0, temperature  $\sim 30\text{ }^{\circ}\text{C}$ , isotonic).

### **MR methods and data analysis**

A 4.7 T preclinical MR-imaging and spectroscopy system (Agilent Technologies, ApS, Santa Clara, CA, USA) was used for the MR-experiments. The rats were placed supine in a  $^{13}\text{C}/^1\text{H}$  radiofrequency (RF) volume coil, and either a  $^{13}\text{C}$  circular receive surface coil or a  $^{13}\text{C}$  four channel receive array coil was placed over the heart (all coils from RAPID Biomedical GmbH, Germany). The inner diameter of the volume coil was 72 mm. The diameter of the surface coil was 20 mm. The array coil consisted of 4 elements of length 42.5 mm and was sensitive to a depth of approximately 20 mm. The surface coil was sensitive to a depth of approximately 15 mm into the animal. The coil profiles are presented in figure 2. Anatomical long axis proton MR-images were acquired for spatial localization of the heart using a cardiac and respiratory-gated cine pulse sequence (TR = 195 ms; TE = 3 ms; FOV = 60 x 120 mm<sup>2</sup>; Slice thickness = 2 mm; Matrix size = 128 x 256, Number of cardiac phases = 8). The position of the coils was verified by an external marker (oil pellet) placed on the top and in the centre of the surface coil. On the array coil, the oil pellet was placed on one side of the coil and the animal was placed so the most sensitive part of the coil was closest to the heart. 1.0 mL hyperpolarized [ $1\text{-}^{13}\text{C}$ ]pyruvate was injected over 7-10 s via the tail vein catheter. 7 s after end of injection, an ECG and respiratory-gated slice-selective a chemical shift imaging (CSI) sequence was started (Slice thickness = 5 mm, flip angle = 10°, Circular spiral  $k$ -space trajectory matrix with 144 phase encoding steps, TR = 69 ms TE = 1.86 ms, FOV = 25 x 25 mm<sup>2</sup>) from the same long axis slice through the heart as the one used for the proton cine imaging. The [ $1\text{-}^{13}\text{C}$ ]pyruvate, [ $1\text{-}^{13}\text{C}$ ]lactate, [ $1\text{-}^{13}\text{C}$ ]alanine and [ $^{13}\text{C}$ ]bicarbonate signals were quantified and mapped using in house written MATLAB scripts (The Mathworks, Natick MA). The spatial dimensions were apodized and zero-filled to a matrix size of 32x32. The spectral analysis was performed by integrating the metabolic signals at predefined frequency offsets relative to the frequency of the pyruvate

peak. The CSI data were presented as metabolic maps, which were registered to the corresponding first cardiac phase proton cine image.

The effect of ischemia was quantified by line profile measurements of the metabolite signals. A line was drawn from the apex along the anterior wall of the myocardium on the cine image covering both the healthy part (proximal) and the ischemic part (distal) of the myocardium. A typical example of how the line was placed on the first cardiac phase proton cine image is shown in figure 3A and 3B (column 5) as well as on the metabolic maps in figure 3C (column 1-4). The metabolite signal values from the corresponding voxels on the metabolite maps were collected and normalized to the maximal signal along the measured line profile (100%). The signals were plotted as a function of the distance from apex (mm) for each animal pre-ischemia and post-ischemia. The distance from where the signal reached 50% of maximum was used for comparison between healthy (pre-ischemia) and diseased (post-ischemia) hearts.

In 7 rats the infarct area was also verified by comparing the metabolic maps visually with proton LE images. ECG-gated inversion recovery gradient echo MR images were obtained 10-20 minutes after the injection of 0.3 mmol/kg gadolinium based contrast agent (Dotarem, Guerbet, USA). The inversion time was adjusted individually for each rat (350-500 ms) to obtain the best contrast between the gadolinium enhanced tissue and the surrounding healthy tissue (TR = 600 ms; TE = 10 ms; FOV = 60 x 120 mm<sup>2</sup>; Slice thickness = 2 mm; Matrix size = 192 x 512).

### **Statistics:**

Paired two-tailed student t-test was performed to evaluate the difference between group mean values from the line profile evaluation pre and post ischemia, for both [ $1\text{-}^{13}\text{C}$ ]alanine and [ $1\text{-}^{13}\text{C}$ ]lactate. Statistical significance was considered at the  $p \leq 0.05$  level.

## **Results**

Figure 3 shows the metabolic images from the hyperpolarized  $^{13}\text{C}$  MRS studies in a rat before

and after 30 min ischemia. Hyperpolarized signal from [1-<sup>13</sup>C]pyruvate, [1-<sup>13</sup>C]lactate, [1-<sup>13</sup>C]alanine and [<sup>13</sup>C]bicarbonate was detected in the hearts of all animals pre-ischemia (figure 3A; Column 1-4). Signal from [1-<sup>13</sup>C]pyruvate was primarily detected from blood inside the ventricle (Figure 3A; Column 1). Signal from [1-<sup>13</sup>C]lactate, [1-<sup>13</sup>C]alanine and [<sup>13</sup>C]bicarbonate was confined primarily to the anterior wall of the myocardium closest to the coil (figure 3A; column 2-4). Low or no <sup>13</sup>C signal was observed from the posterior myocardial wall. Signal loss was observed in the metabolic images from the outer part of the apex both pre- and post-ischemia (Figure 3A and B). Loss of signal from the other part of apex was also observed on the proton cine images, which corresponded with the loss of signal in the metabolic images (figure 3A and B; column 5).

Using the line profile comparison a significant decrease was observed in the [1-<sup>13</sup>C]alanine signal in the distal region of the anterior wall (ischemic region) post-ischemia compared to pre-ischemia (figure 4). The distance for which the [1-<sup>13</sup>C]alanine signal reached 50% of max was 2.3 mm ± 0.43 mm (mean ± standard error) pre-ischemia and 6.4 mm ± 1.0 mm (mean ± standard error) post-ischemia with a difference of 4.1 mm (CI-95%, p = 0.0053) (figure 5A). Elevated signal in the late-enhancement images was observed in the area, which showed reduced <sup>13</sup>C signal in the [1-<sup>13</sup>C]alanine maps (figure 3C; Column 5). A smaller difference in mean distance between pre- and post-ischemia was detected in the [1-<sup>13</sup>C]lactate signal level than in the [1-<sup>13</sup>C]alanine signal level (figure 5B), but the difference was still significant. The mean distance for which the [1-<sup>13</sup>C]lactate signal reached 50% of max was 1.4 mm ± 0.45 mm (mean ± standard error) pre-ischemia and 3.6 mm ± 0.79 mm (mean ± standard error) post-ischemia with a difference of 2.2 mm (CI-95%, p = 0.042). The overall signal from [<sup>13</sup>C]bicarbonate was often under the limit of detection post-ischemia both in the ischemic area and the surrounding healthy tissue (figure 3B, Column 4).

Troponin I blood levels were only measured post ischemia in 6 out of 10 rats due to problems with the blood drawing during

scanning. In two animals the last sample was taken approximately 3 hours after reperfusion when the rat was removed from the scanner. The results are shown in figure 6. The Troponin I level peaked 1 hour after reperfusion and continued to be elevated 2-3 hours after reperfusion. The mean value of Troponin I one hour after reperfusion was 41.0 ng/mL ± 13.2 ng/mL (mean ± standard deviation) in the infarcted group and 0.13 ng/mL and 0.93 ng/mL in the two sham operated rats respectively.

## Discussion

This study demonstrates that regional metabolic changes following myocardial ischemia can be assessed in rats in vivo using hyperpolarized <sup>13</sup>C MRS. The decrease in [1-<sup>13</sup>C]alanine and [1-<sup>13</sup>C]lactate signal from the ischemic area confirms that the ischemic insult was severe, as it reflects an overall depression of the cellular metabolism. The increase in the blood levels of Troponin I also suggests that the ischemic insult is severe as Troponin I is released to the blood as a result of myocardial tissue damage (19). A decrease in [<sup>13</sup>C]bicarbonate signal was also expected since the mitochondrial activity and especially PDH enzyme activity is very sensitive to ischemia (1, 7, 20). However, the overall level of [<sup>13</sup>C]bicarbonate signal was often under the limit of detection post-ischemia. It is known that, during tissue acidic conditions, which is typical for ischemia, the CA enzyme activity is decreased (21), which would affect the generation of [<sup>13</sup>C]bicarbonate from <sup>13</sup>CO<sub>2</sub> (assuming the end metabolic product in PDH is CO<sub>2</sub> and not bicarbonate). However, in this study acidosis is not believed to affect the measurements, because the hyperpolarized MRS scanning is performed after 2 hours of reperfusion during which time the acidosis is expected to be re-regulated. Furthermore, no [<sup>13</sup>C]bicarbonate signal could be detected in the healthy (non ischemic) part of the myocardium post-ischemia either, and here an intact CA enzyme activity would be expected including an intact [<sup>13</sup>C]bicarbonate production. Therefore, we hypothesize that the reduced [<sup>13</sup>C]bicarbonate signal post-ischemia is the consequence of a generalized low cardiac PDH-activity in the rat heart, probably as consequence of a shift in the substrate

metabolism towards free fatty acids (FFA) as discussed in the following.

It is known that glucose and FFA compete as substrates for energy production in the heart. Especially during fasting the glucose metabolism declines, FFA utilisation goes up and PDH activity decreases (20, 22, 23). The post-ischemic condition could mimic a “fasted” or rather an “un-fed” situation, because the rat has been anesthetised for a long time before scanning, and this could more likely be the explanation for the overall low [ $^{13}\text{C}$ ]bicarbonate signal observed post-ischemia. Decrease or absence of bicarbonate as a response to ischemia is not directly associated with cell death, but indicates that the flux through the PDH enzyme and the mitochondrial activity has decreased. This effect can be recovered after a while, when the blood flow is re-established, which in principle can be used to determine the severity of the ischemic insult by hyperpolarized  $^{13}\text{C}$  MRS, as it was demonstrated in the pig hearts by Golman et al (13). So if a complete evaluation of the severity of the ischemia is required, the information from [ $^{13}\text{C}$ ]bicarbonate is important. High [ $^{13}\text{C}$ ]bicarbonate signal might be achieved by using coils with a higher sensitivity. Other ways would be to increase the overall glucose oxidation and flux through PDH in the heart by ensure a fully (carbohydrate rich) fed condition at the time of scanning or by infusion of a mixture of glucose, insulin and potassium (GIK) or treatment with the PDH-kinase inhibitor dichloroacetic acid (DCA), which both has shown to enhance the PDH-flux in hyperpolarized MRS studies in rat hearts (10, 24, 25). Ischemia is commonly associated with elevated lactate levels, as LDH activity is known to be increased under anaerobic conditions, which also has been demonstrated previously in hyperpolarized  $^{13}\text{C}$  MRS studies in isolated rat hearts (7, 12). However, a small decrease was observed between ischemic and healthy hearts in this study. Lactate produced in the surrounding damaged tissue, superimposed over or folded into the myocardium could affect the measurements post-ischemia. Lactate signal from the damaged chest wall can be observed in the metabolic maps and in the blood inside the ventricle (figure 3B; column 2). Another explanation could be variation in the severity of

ischemia. The balance between prolonged anaerobic condition (increased LDH activity) and the progression to cell death (reduced LDH activity) is not yet fully understood.

Two different coils were used in this study, but the same coil was always used pre- and post-ischemia in the same animal. The reason for using two coils was to evaluate their sensitivity and coverage of the heart. However, optimal coverage was not achieved by any of the coils (low  $^{13}\text{C}$  signal was detected from the posterior myocardial wall using both coils). Data from both coils was therefore included in the study since the coil is not believed to affect the line profile evaluation pre- and post-ischemia. As described in the results section, signal loss was observed from the outer part of the apex, which could not be explained by the sensitivity of the coils. It may be explained by a susceptibility effect caused by the lung parenchyma, since loss of signal from the apex also was observed on the proton cine-images.

The variation in the Troponin I signal could be due to variation in the infarct size (placement of the ligature) and variation in the cellular injury that takes place between LAD occlusion and blood sampling. Histological analysis of the heart was not included in this study, because the model was considered too acute to observe macroscopic changes. However, histological stainings of the myocardium could be a valuable addition for future hyperpolarized  $^{13}\text{C}$  MRS studies in rats.

## Conclusion

After i.v. injection of hyperpolarized [ $1-^{13}\text{C}$ ]pyruvate, signal from [ $1-^{13}\text{C}$ ]pyruvate, [ $1-^{13}\text{C}$ ]lactate, [ $1-^{13}\text{C}$ ]alanine and [ $^{13}\text{C}$ ]bicarbonate could be detected in the in vivo rat heart pre-ischemia and localized metabolic images could be produced of the anterior part of the heart. After 30 min occlusion of the LAD and 2 hours of reperfusion a decrease in the signal of [ $1-^{13}\text{C}$ ]alanine and [ $1-^{13}\text{C}$ ]lactate was observed in the ischemic region of the hearts, whereas the [ $^{13}\text{C}$ ]bicarbonate signal hardly could be detected in hearts post-ischemia. Concomitant increase in the blood levels of Troponin I could be detected and enhanced gadolinium signal using late enhancement MRI was observed. The decrease

in the [1-<sup>13</sup>C]alanine and [1-<sup>13</sup>C]lactate signal in the ischemic area confirms that the ischemic insult is severe, as it reflects an overall depression of the cellular metabolism, which is in agreement with previous animal studies of cardiac metabolism with hyperpolarized [1-<sup>13</sup>C]pyruvate MRS. To our knowledge this is the first time in ischemic rat hearts that regional metabolic changes have been imaged in vivo using hyperpolarized <sup>13</sup>C MRI. The advantage of the in vivo rat model is that it offers the possibility to study cardiac metabolism in a more natural biological environment than isolated heart models. The combination of hyperpolarized MRS and the in vivo ischemic rat model enables new possibilities to evaluate changes in metabolism both before and after ischemia and may contribute with important knowledge for the potential application of the technique in humans.

## References

- Opie LH. Metabolism of free fatty acids, glucose and catecholamines in acute myocardial infarction. Relation to myocardial ischemia and infarct size. *Am J Cardiol* 1975;36:938-953.
- Aguor EN, van de Kolk CW, Arslan F, Nederhoff MG, Doevendans PA, Pasterkamp G, Strijkers GJ, van Echteld CJ. <sup>23</sup>Na chemical shift imaging and Gd enhancement of myocardial edema. *Int J Cardiovasc Imaging* 2013;29:343-354.
- Schneider JE, Tyler DJ, Ten HM, Sang AE, Cassidy PJ, Fischer A, Wallis J, Sebag-Montefiore LM, Watkins H, Isbrandt D, Clarke K, Neubauer S. In vivo cardiac 1H-MRS in the mouse. *Magn Reson Med* 2004;52:1029-1035.
- Tyler DJ, Hudsmith LE, Clarke K, Neubauer S, Robson MD. A comparison of cardiac <sup>31</sup>P MRS at 1.5 and 3 T. *NMR Biomed* 2008;21:793-798.
- Carvalho RA, Zhao P, Wiegers CB, Jeffrey FM, Malloy CR, Sherry AD. TCA cycle kinetics in the rat heart by analysis of <sup>13</sup>C isotopomers using indirect <sup>1</sup>H. *Am J Physiol Heart Circ Physiol* 2001;281:1413-1421.
- Ziegler A, Zaugg CE, Buser PT, Seelig J, Kunnecke B. Non-invasive measurements of myocardial carbon metabolism using in vivo <sup>13</sup>C NMR spectroscopy. *NMR Biomed* 2002;15:222-234.
- Schroeder MA, Atherton HJ, Ball DR, Cole MA, Heather LC, Griffin JL, Clarke K, Radda GK, Tyler DJ. Real-time assessment of Krebs cycle metabolism using hyperpolarized <sup>13</sup>C magnetic resonance spectroscopy. *FASEB J* 2009;23:2529-2538.
- Ardenkjaer-Larsen JH, Fridlund B, Gram A, Hansson G, Hansson L, Lerche MH, Servin R, Thaning M, Golman K. Increase in signal-to-noise ratio of > 10,000 times in liquid-state NMR. *Proc Natl Acad Sci U S A* 2003;100:10158-10163.
- Bing RJ, Siegel A, Vitale A, Balboni F, Sparks E, Taeschler M, Klapper M, Edwards S. Metabolic studies on the human heart in vivo. I. Studies on carbohydrate metabolism of the human heart. *Am J Med* 1953;15:284-296.
- Atherton HJ, Schroeder MA, Dodd MS, Heather LC, Carter EE, Cochlin LE, Nagel S, Sibson NR, Radda GK, Clarke K, Tyler DJ. Validation of the in vivo assessment of pyruvate dehydrogenase activity using hyperpolarised <sup>13</sup>C MRS. *NMR Biomed* 2011;24:201-208.
- Merritt ME, Harrison C, Storey C, Jeffrey FM, Sherry AD, Malloy CR. Hyperpolarized <sup>13</sup>C allows a direct measure of flux through a single enzyme-catalyzed step by NMR. *Proc Natl Acad Sci U S A* 2007;104:19773-19777.
- Ball DR, Cruickshank R, Carr CA, Stuckey DJ, Lee P, Clarke K, Tyler DJ. Metabolic imaging of acute and chronic infarction in the perfused rat heart using hyperpolarised [1-<sup>13</sup>C]pyruvate. *NMR Biomed* 2013;26:1441-1450.
- Golman K, Petersson JS, Magnusson P, Johansson E, Akeson P, Chai CM, Hansson G, Mansson S. Cardiac

- metabolism measured noninvasively by hyperpolarized <sup>13</sup>C MRI. *Magn Reson Med* 2008;59:1005-1013.
14. Lau AZ, Chen AP, Ghugre NR, Ramanan V, Lam WW, Connelly KA, Wright GA, Cunningham CH. Rapid multislice imaging of hyperpolarized <sup>13</sup>C pyruvate and bicarbonate in the heart. *Magn Reson Med* 2010;64:1323-1331.
  15. Schroeder MA, Clarke K, Neubauer S, Tyler DJ. Hyperpolarized magnetic resonance: a novel technique for the in vivo assessment of cardiovascular disease. *Circulation* 2011;124:1580-1594.
  16. Nelson SJ, Kurhanewicz J, Vigneron DB, Larson PE, Harzstark AL, Ferrone M, van CM, Chang JW, Bok R, Park I, Reed G, Carvajal L, Small EJ, Munster P, Weinberg VK, Ardenkjaer-Larsen JH, Chen AP, Hurd RE, Odegardstuen LI, Robb FJ, Tropp J, Murray JA. Metabolic Imaging of Patients with Prostate Cancer Using Hyperpolarized [1-<sup>13</sup>C]Pyruvate. *Sci Transl Med* 2013;5:198ra108.
  17. Johns TN, Olson BJ. Experimental myocardial infarction. I. A method of coronary occlusion in small animals. *Ann Surg* 1954;140:675-682.
  18. Ye J, Yang L, Sethi R, Copps J, Ramjiawan B, Summers R, Deslauriers R. A new technique of coronary artery ligation: experimental myocardial infarction in rats in vivo with reduced mortality. *Mol Cell Biochem* 1997;176:227-233.
  19. Tiwari RP, Jain A, Khan Z, Kohli V, Bharmal RN, Kartikeyan S, Bisen PS. Cardiac troponins I and T: molecular markers for early diagnosis, prognosis, and accurate triaging of patients with acute myocardial infarction. *Mol Diagn Ther* 2012;16:371-381.
  20. Patel MS, Korotchkina LG. Regulation of the pyruvate dehydrogenase complex. *Biochem Soc Trans* 2006;34:217-222.
  21. Khalifah RG. The carbon dioxide hydration activity of carbonic anhydrase. I. Stop-flow kinetic studies on the native human isoenzymes B and C. *J Biol Chem* 1971;246:2561-2573.
  22. Neely JR, Morgan HE. Relationship between carbohydrate and lipid metabolism and the energy balance of heart muscle. *Annu Rev Physiol* 1974;36:413-459.
  23. Stanley WC, Recchia FA, Lopaschuk GD. Myocardial substrate metabolism in the normal and failing heart. *Physiol Rev* 2005;85:1093-1129.
  24. Lauritzen MH, Laustsen C, Butt SA, Magnusson P, Sogaard LV, Ardenkjaer-Larsen JH, Akeson P. Enhancing the [<sup>13</sup>C]bicarbonate signal in cardiac hyperpolarized [1-<sup>13</sup>C]pyruvate MRS studies by infusion of glucose, insulin and potassium. *NMR Biomed* 2013;26:1496-1500.
  25. Atherton HJ, Dodd MS, Heather LC, Schroeder MA, Griffin JL, Radda GK, Clarke K, Tyler DJ. Role of pyruvate dehydrogenase inhibition in the development of hypertrophy in the hyperthyroid rat heart: a combined magnetic resonance imaging and hyperpolarized magnetic resonance spectroscopy study. *Circulation* 2011;123:2552-2561.

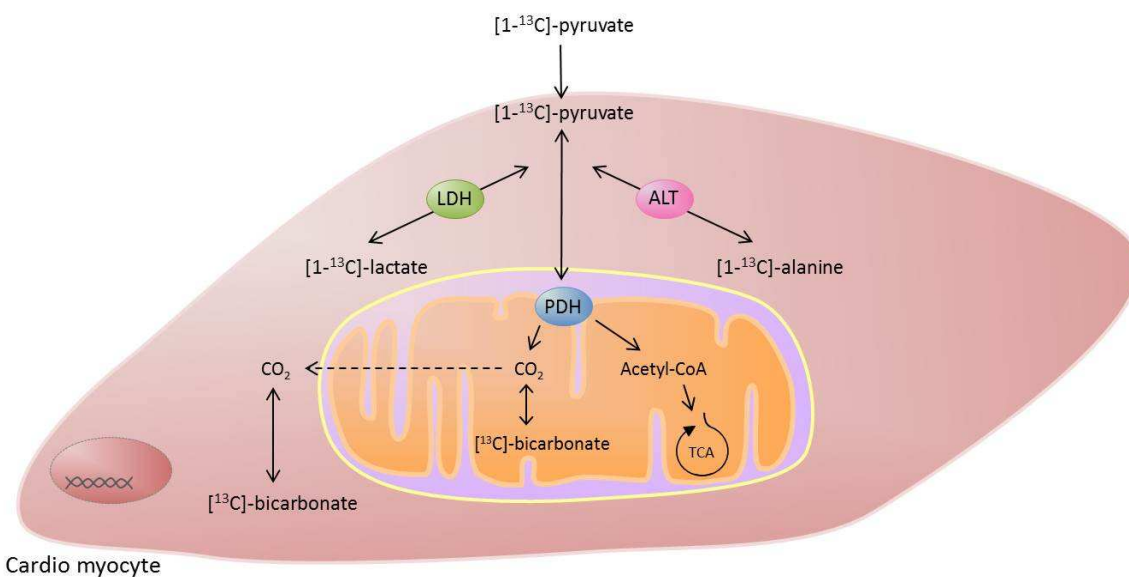


**Figure 1.** When injected i.v.  $[1-^{13}\text{C}]$ pyruvate is taken up by the cardio myocytes and converted into  $[1-^{13}\text{C}]$ lactate via the enzyme lactate dehydrogenase (LDH) and  $[1-^{13}\text{C}]$ alanine via alanine aminotransferase (ALT) in the cytosol.  $[1-^{13}\text{C}]$ pyruvate is also converted into Acetyl CoA via the pyruvate dehydrogenase (PDH) complex in the mitochondrial membrane. In the process  $[^{13}\text{C}]$ bicarbonate is produced via  $^{13}\text{CO}_2$  and the enzyme carbonic anhydrase (CA). Acetyl CoA is one of the main fuels for production of energy in the TCA-cycle.

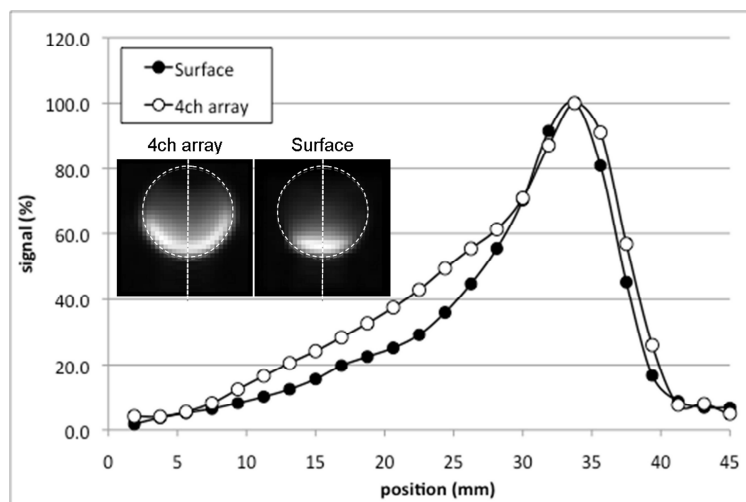


**Figure 2.** Sensitivity profiles of the circular surface receive coil and the 4 channel array receive coil are compared. The sensitivity was measured using a spherical phantom containing unpolarized  $[1-^{13}\text{C}]$ pyruvate. The signals are normalized to their maximum (100%). The 4 channel array coil is sensitive to a depth of ~20 mm. The surface coil is sensitive to a depth of ~15 mm into the animal. Thus, the array coil has a slightly better coverage than the surface coil.

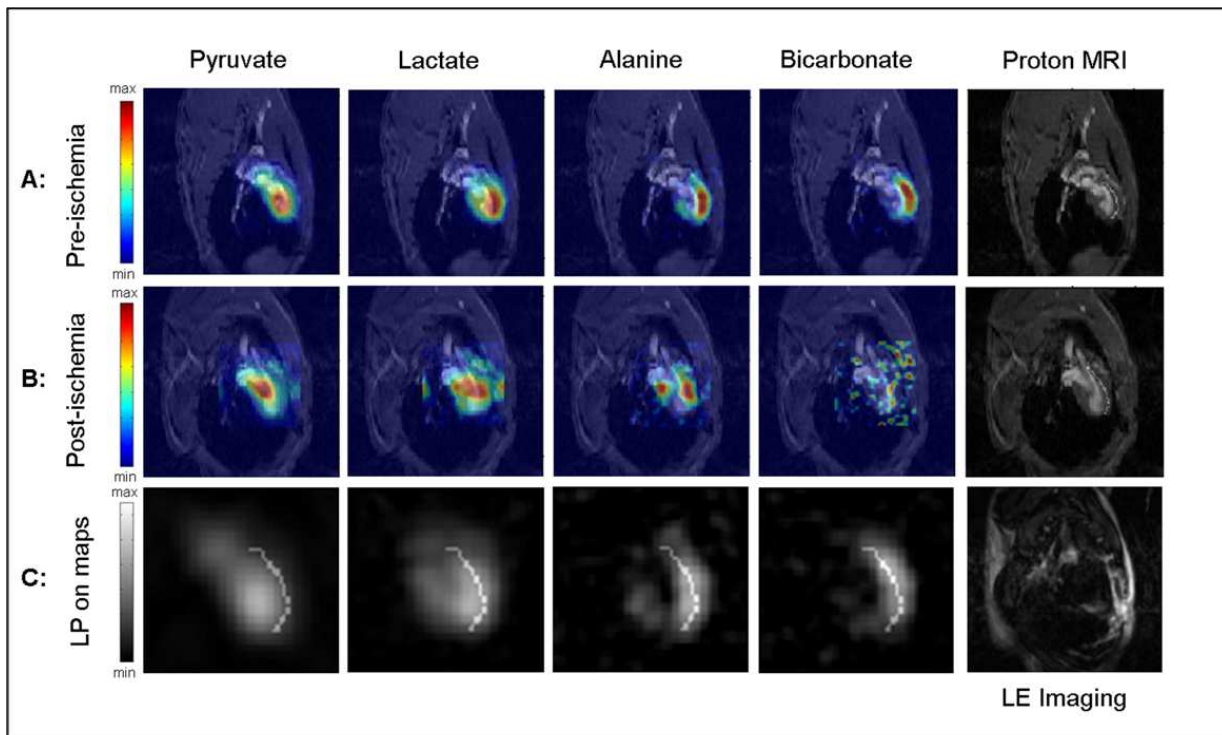


**Figure 3.** Representative metabolic images of cardiac metabolism (A) pre-ischemia (healthy heart) and (B) post-ischemia (30 min ischemia followed by 2 hours reperfusion) for  $[1-^{13}\text{C}]$ pyruvate,  $[1-^{13}\text{C}]$ lactate,  $[1-^{13}\text{C}]$ alanine and  $[^{13}\text{C}]$ bicarbonate respectively (FOV = 25 x 25 mm, slice thickness = 5 mm, FA = 10°). The proton MRI (last column to the right) shows an example of how the line used for the line profile (LP) analysis is drawn on the proton cine-images. (C) Shows the LP as overlay on the metabolic maps pre-ischemia in black and white. The corresponding post-ischemia late enhancement (LE) image is shown down in the right corner. Enhanced signal can be observed in the distal ischemic region of the anterior myocardial wall including in the tissue of the anterior chest wall.

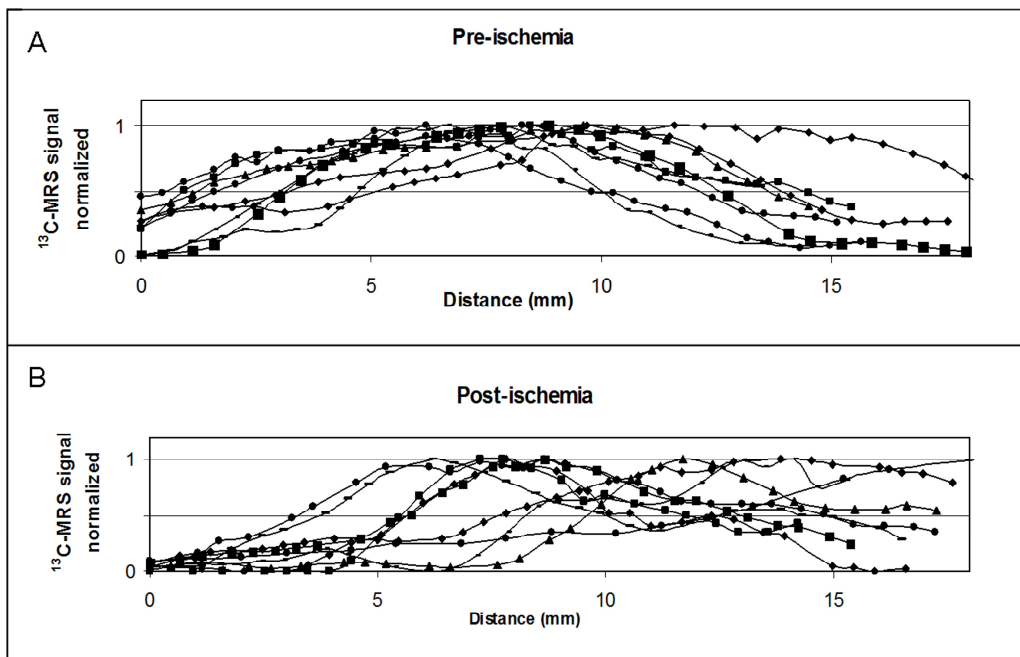


**Figure 4.** Line profiles drawn on the anterior wall of the myocardium for  $[1-^{13}\text{C}]$ alanine. The signals were plotted as distance from apex (mm) for each animal (A) pre-ischemia and (B) post-ischemia. The mean distance for which the  $[1-^{13}\text{C}]$ alanine signal reached 50% was used to compare signal differences between pre-ischemic and post-ischemic hearts seen in figure 5.

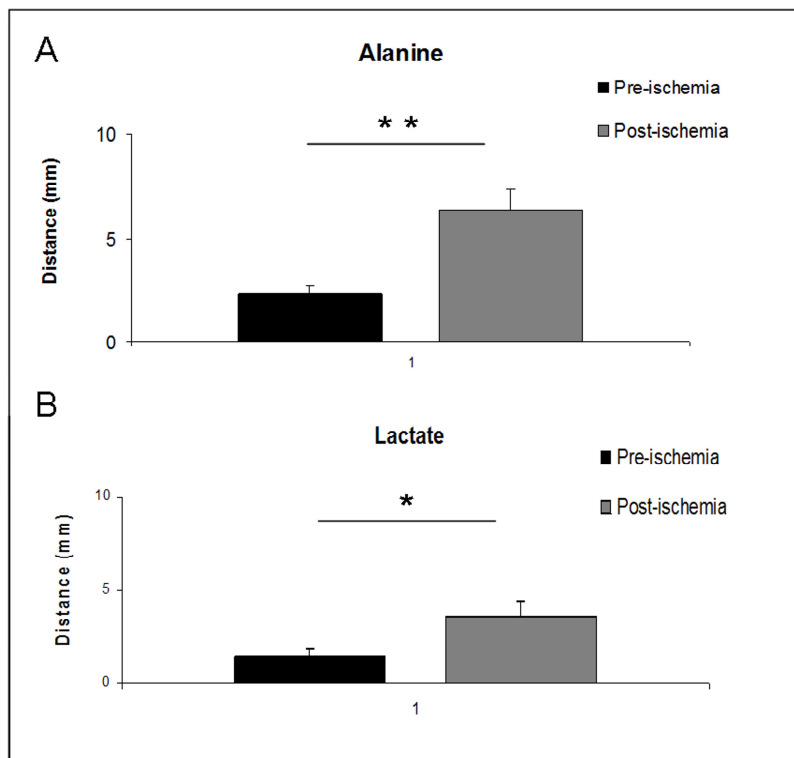


**Figure 5.** Mean distances from the line profile analysis of (A) [1-<sup>13</sup>C]alanine and (B) [1-<sup>13</sup>C]lactate. The mean distance for which the signal reached 50% is significant longer post-ischemia compared to pre-ischemia for both [1-<sup>13</sup>C]alanine and [1-<sup>13</sup>C]lactate (\*\* p < 0.01, \* p < 0.05).

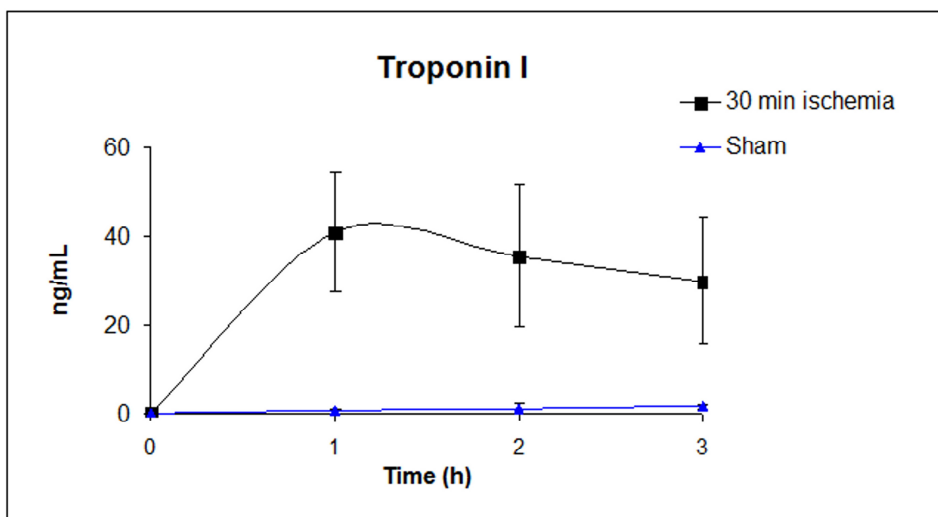


**Figure 6.** Blood levels of Troponin I measured pre-ischemia (0 hours) and 1,2 and 3 hours after reperfusion in ischemic (n = 7) and sham operated rats (n = 2). The Troponin I level peaked after 1 hour of reperfusion (41.0 ng/mL ± 13.2 ng/mL (mean ± SD) in the ischemic rats).

## **PAPER II**

# Enhancing the [ $^{13}\text{C}$ ]bicarbonate signal in cardiac hyperpolarized [ $1\text{-}^{13}\text{C}$ ]pyruvate MRS studies by infusion of glucose, insulin and potassium

Mette Hauge Lauritzen<sup>a\*</sup>, Christoffer Laustsen<sup>a,b</sup>, Sadia Asghar Butt<sup>a</sup>, Peter Magnusson<sup>a</sup>, Lise Vejby Søgaard<sup>a</sup>, Jan Henrik Ardenkjær-Larsen<sup>a,c,d</sup> and Per Åkeson<sup>a</sup>

A change in myocardial metabolism is a known effect of several diseases. MRS with hyperpolarized  $^{13}\text{C}$ -labelled pyruvate is a technique capable of detecting changes in myocardial pyruvate metabolism, and has proven to be useful for the evaluation of myocardial ischaemia *in vivo*. However, during fasting, the myocardial glucose oxidation is low and the fatty acid oxidation ( $\beta$ -oxidation) is high, which complicates the interpretation of pyruvate metabolism with the technique. The aim of this study was to investigate whether the infusion of glucose, insulin and potassium (GIK) could increase the myocardial glucose oxidation in the citric acid cycle, reflected as an increase in the [ $^{13}\text{C}$ ]bicarbonate signal in cardiac hyperpolarized [ $1\text{-}^{13}\text{C}$ ]pyruvate MRS measurements in fasted rats. Two groups of rats were infused with two different doses of GIK and investigated by MRS after injection of hyperpolarized [ $1\text{-}^{13}\text{C}$ ]pyruvate. No [ $^{13}\text{C}$ ]bicarbonate signal could be detected in the fasted state. However, a significant increase in the [ $^{13}\text{C}$ ]bicarbonate signal was observed by the infusion of a high dose of GIK. This study demonstrates that a high [ $^{13}\text{C}$ ]bicarbonate signal can be achieved by GIK infusion in fasted rats. The increased [ $^{13}\text{C}$ ]bicarbonate signal indicates an increased flux of pyruvate through the pyruvate dehydrogenase enzyme complex and an increase in myocardial glucose oxidation through the citric acid cycle. Copyright © 2013 John Wiley & Sons, Ltd.

**Keywords:** hyperpolarization;  $^{13}\text{C}$ ; MRS; cardiac metabolism; pyruvate dehydrogenase; glucose; insulin

## INTRODUCTION

The heart has the capability to utilise a variety of different substrates for energy production, such as glucose, fatty acids (FAs), lactate and ketone bodies. Under normal conditions, FAs, catabolised by  $\beta$ -oxidation, account for 60–90% of the total myocardial energy production, whereas glucose metabolised through glycolysis accounts for 10–40% of total energy production (1–3). Several diseases can be characterised by alterations in myocardial substrate metabolism, such as diabetes, hyperthyroidism, ischaemic heart disease and heart failure (4–7). Thus, there is great interest in developing new methods for the evaluation of these metabolic changes.

MRS using hyperpolarized  $^{13}\text{C}$ -labelled pyruvate is a technique capable of detecting changes in myocardial metabolism (8,9). After injection, hyperpolarized [ $1\text{-}^{13}\text{C}$ ]pyruvate is taken up by the cells and the metabolic conversion of [ $1\text{-}^{13}\text{C}$ ]pyruvate to [ $1\text{-}^{13}\text{C}$ ]lactate, [ $1\text{-}^{13}\text{C}$ ]alanine and [ $^{13}\text{C}$ ]bicarbonate through specific enzymes can be detected in real time (10–12). The pyruvate dehydrogenase (PDH) enzyme complex catalyses the irreversible oxidation of pyruvate into acetyl-CoA and  $\text{CO}_2$  (in equilibrium with bicarbonate) in the mitochondria. Acetyl-CoA enters the citric acid cycle for the generation of ATP. Thus, the production of [ $^{13}\text{C}$ ]bicarbonate in hyperpolarized  $^{13}\text{C}$  MRS studies represents the flux of pyruvate through PDH and the supply of acetyl-CoA from the glycolytic pathway to the citric acid cycle (11). The

activity of PDH is tightly regulated. PDH is inactivated by PDH kinase (PDK) and reactivated by PDH phosphatase (PDP). High intramitochondrial concentration of acetyl-CoA and nicotinamide

\* Correspondence to: M. H. Lauritzen, Copenhagen University Hospital Hvidovre, Kettegårds Allé 30, 2650 Hvidovre, Denmark  
E-mail: metteh@drcmr.dk

a M. H. Lauritzen, C. Laustsen, S. A. Butt, P. Magnusson, L. V. Søgaard, J. H. Ardenkjær-Larsen, P. Åkeson  
Danish Research Centre for Magnetic Resonance (DRCMR), Copenhagen University Hospital Hvidovre, Hvidovre, Denmark

b C. Laustsen  
MR Research Centre, Institute of Clinical Medicine, Aarhus University Hospital, Aarhus, Denmark

c J. H. Ardenkjær-Larsen  
GE Healthcare, Brøndby, Denmark

d J. H. Ardenkjær-Larsen  
Technical University of Denmark, Department of Electrical Engineering, Kgs Lyngby, Denmark

**Abbreviations used:** ANOVA, analysis of variance; CI, confidence interval; CSI, chemical shift imaging; DCA, dichloroacetic acid; FA, fatty acid; GIK, glucose, insulin and potassium; NADH, nicotinamide adenine dinucleotide hydride; PDH, pyruvate dehydrogenase; PDK, pyruvate dehydrogenase kinase; PDP, pyruvate dehydrogenase phosphatase; PET, positron emission tomography.

adenine dinucleotide hydride (NADH) stimulates PDK, resulting in PDH inhibition (negative feedback) (13,14). During fasting, when the blood glucose level is low, FAs are released into the blood from adipose tissue and hepatic triglyceride stores. FAs are also converted to acetyl-CoA via mitochondrial  $\beta$ -oxidation, and thereby compete with glucose to enter the citric acid cycle via acetyl-CoA. As a result, PDH is inactivated and FA metabolism increases. In contrast, insulin is known to stimulate PDP, thereby reactivating PDH and inhibiting FA metabolism. Insulin also stimulates glucose uptake and increases glycolysis, which leads to increased levels of pyruvate that inhibit PDK, and thereby stimulate PDH indirectly (5,13,15). Up- or down-regulation of myocardial PDH activity has been observed in several disease states (4–7), and the assessment of these metabolic changes could potentially allow earlier diagnosis or the monitoring of response to treatment.

In patients with acute myocardial infarction, a rapid increase in plasma FA is observed in the first 1–2 h after the onset of symptoms (16). The elevated level of FA is believed to worsen the ischaemic damage to the myocardium (17). The infusion of glucose, insulin and potassium (GIK) is able to decrease the circulating FA levels, and is believed to have a direct protective effect on ischaemic tissue (18). GIK infusions have therefore been studied extensively as therapy in patients with myocardial infarction (19). In positron emission tomography (PET) studies, GIK has been shown to increase the uptake of the radioactive fluorine-18-labelled glucose analogue, [ $^{18}\text{F}$ ]FDG, to maintain a metabolic steady state during scanning and to improve image quality (20,21), whereas fasting prior to PET scanning yields heterogeneous [ $^{18}\text{F}$ ]FDG uptake and poor image quality (22,23). The effect of fasting on the hyperpolarized  $^{13}\text{C}$  MRS signal has recently been examined *in vivo* by Schroeder *et al.* (9). Low myocardial [ $^{13}\text{C}$ ]bicarbonate signal was observed in fasted rats after [ $1\text{-}^{13}\text{C}$ ]pyruvate injection, relative to fed rats, indicating a low flux of [ $1\text{-}^{13}\text{C}$ ]pyruvate through PDH. Furthermore, hyperpolarized  $^{13}\text{C}$  MRS studies in perfused hearts have shown that hearts exposed to substrates mimicking a fasted state resulted in a 60% reduction of [ $1\text{-}^{13}\text{C}$ ]pyruvate utilization relative to the fed state (24). These studies stress the importance of ensuring a fed condition when measuring cardiac metabolism with hyperpolarized [ $1\text{-}^{13}\text{C}$ ]pyruvate. However, controlling the feeding condition can be difficult, especially if the animal has been anaesthetised for a long period of time. Similar challenges can be expected if the hyperpolarized  $^{13}\text{C}$  MRS technique is translated into clinical use in heart patients. The optimal situation for a cardiac experiment with hyperpolarized [ $1\text{-}^{13}\text{C}$ ]pyruvate would be a metabolic state with high PDH activity.

The aim of this study was to examine the effect of GIK infusion on cardiac metabolism by hyperpolarized  $^{13}\text{C}$  MRS in fasted rats. We hypothesise that the infusion of GIK will increase the myocardial glucose oxidation through the citric acid cycle, and thereby increase the signal from [ $^{13}\text{C}$ ]bicarbonate in fasted rat hearts.

## MATERIALS AND METHODS

### Animals, anaesthesia and general procedures

Twelve male Sprague Dawley rats (250–300 g) were fasted overnight (12–16 h) and anaesthetised with 4% isoflurane and maintained with 1.8% isoflurane mixed with air and 25% oxygen. Two tail vein catheters were inserted, one for the infusion of GIK and the other for the administration of hyperpolarized [ $1\text{-}^{13}\text{C}$ ]pyruvate. The potassium limits hypokalaemia during infusion. A

third catheter was inserted in the left femoral artery for the collection of blood during scanning. The rats were intubated for artificial respiration (70 breaths/min), and temperature and expiration gases were monitored (body temperature, 37.0–38.0 °C; expiration  $\text{CO}_2$ , 3.5–4.0 kPa).

The rats were randomly separated into two groups. The first group ( $n=6$ ) was infused for 1 h with a high dose of GIK (25 mg/kg/min glucose, 5 mU/kg/min insulin and 10 mmol/kg/min potassium). The second group ( $n=5$ ) received a lower dose (15 mg/kg/min glucose, 3 mU/kg/min insulin and 10 mmol/kg/min potassium). The insulin was a fast-acting type (Actrapid, Novo Nordisk A/S, Bagsvaerd, Denmark). The rats were scanned three times with hyperpolarized [ $1\text{-}^{13}\text{C}$ ]pyruvate: (i) in the fasted state; (ii) immediately after the infusion of GIK; and (iii) 1 h after GIK infusion. Prior to each scan, blood was collected for blood glucose measurements (OneTouch Ultra 2, LifeScan, Birkerød, Denmark).

### $^{13}\text{C}$ polarization

The [ $1\text{-}^{13}\text{C}$ ]pyruvic acid (Sigma Aldrich, Brøndby, Denmark.) was mixed with 15 mM trityl radical OX063 (Oxford Instruments, Abingdon, Oxfordshire, UK) and 1.5 mM Dotarem (Guerbet, Villepinte, France). The nuclear hyperpolarization of [ $1\text{-}^{13}\text{C}$ ]pyruvate was performed in a HyperSense polarizer (Oxford Instruments). The polarizer uses the dynamic nuclear polarization technique, described in detail by Ardenkjaer-Larsen *et al.* (25). The polarized samples were dissolved in buffer [80 mM tris(hydroxymethyl)aminomethane, 100 mg/L ethylenediaminetetraacetic acid, 50 mM NaCl, 80 mM NaOH] with the final concentration of 80 mM [ $1\text{-}^{13}\text{C}$ ]pyruvate (pH 7.0–8.0; temperature,  $\sim 30$  °C; isotonic).

### MR methods and data analysis

A 4.7-T preclinical horizontal bore magnet was used for the hyperpolarized  $^{13}\text{C}$  MRS experiments. The magnet was equipped with a Varian Direct Drive console and vnmrj 2.3A software was used for acquisition (Agilent Technologies, Santa Clara, CA, USA). The rats were placed in a  $^{13}\text{C}/^1\text{H}$  radiofrequency volume coil, and a  $^{13}\text{C}$  four-channel array coil (receive-only), with a curved surface, was placed over the heart (both radiofrequency coils from RAPID Biomedical GmbH, Rimpfing, Germany). The inner diameter of the volume coil was 72 mm. The receive channel array consisted of four elements with a length of 42.5 mm with a sensitivity reaching approximately 15–20 mm into the animal. Anatomical long-axis  $^1\text{H}$  MR images were acquired prior to the  $^{13}\text{C}$  MRS scans for the spatial localization of the heart and for the control of correct coil positioning using a cardiac and respiratory-gated Cine pulse sequence. One millilitre of 80 mM hyperpolarized [ $1\text{-}^{13}\text{C}$ ]pyruvate was injected as a bolus injection over 5–8 s. Dynamic  $^{13}\text{C}$  MR spectra were acquired from a nongated long-axis slice to measure metabolism as a function of time (slice thickness, 5 mm; flip angle, 10°; TR = 1 s). The spectra from each of the four coil elements were summed from the maximum pyruvate peak over a 30-s time window (30 spectra) to effectively generate area-under-the-curve signals. The metabolite signals were quantified using the Hankel singular value decomposition method in MATLAB (26), and the data from the coil elements were then combined. The signal (peak area) from [ $^{13}\text{C}$ ]bicarbonate, [ $1\text{-}^{13}\text{C}$ ]alanine and [ $1\text{-}^{13}\text{C}$ ]lactate was normalized to the [ $1\text{-}^{13}\text{C}$ ]pyruvate signal. One animal that received a high dose of GIK was treated as described above, but examined with an cardiac and

a respiratory-gated slice-selective chemical shift imaging (CSI) sequence for metabolic  $^{13}\text{C}$  imaging (Fig. 1B). The CSI images were acquired from a 5-mm-long-axis slice through the heart, similar to that used for dynamic  $^{13}\text{C}$  spectra acquisition (flip angle,  $10^\circ$ ; a spiral trajectory; matrix,  $12 \times 12$ ; TR/TE = 69 ms/1.86 ms; field of view,  $25 \times 25 \text{ mm}^2$ ).

### Statistics

Repeated-measurement analysis of variance (ANOVA) was performed to evaluate the difference between group mean values of  $[1-^{13}\text{C}]\text{alanine}/[1-^{13}\text{C}]\text{pyruvate}$ ,  $[1-^{13}\text{C}]\text{lactate}/[1-^{13}\text{C}]\text{pyruvate}$  ratios and blood glucose values. Because the  $[^{13}\text{C}]\text{bicarbonate}$  signal was below the detection limit in both the fasted and post-GIK states (low dose), single-sample two-tailed  $t$ -tests of mean equal to zero were used to compare differences in the  $[^{13}\text{C}]\text{bicarbonate}/[1-^{13}\text{C}]\text{pyruvate}$  ratio between the fasted state and GIK, and between GIK and post-GIK, in both the low- and high-dose groups. An impaired two-tailed  $t$ -test was used to compare differences in the  $[^{13}\text{C}]\text{bicarbonate}/[1-^{13}\text{C}]\text{pyruvate}$  ratio between the low- and high-dose groups. Statistical significance was considered at the  $p \leq 0.05$  level.

## RESULTS

### $[^{13}\text{C}]\text{Bicarbonate}$ signal

The effect of GIK infusion on the  $[^{13}\text{C}]\text{bicarbonate}$  signal was evaluated. The results are shown in Fig. 1A. No signal from  $[^{13}\text{C}]\text{bicarbonate}$  could be detected after fasting in either group. A high signal from  $[^{13}\text{C}]\text{bicarbonate}$  was detected after the

infusion of GIK in the high-dose group, and the  $[^{13}\text{C}]\text{bicarbonate}/[1-^{13}\text{C}]\text{pyruvate}$  signal ratio was significantly greater than zero (representing the fasted state) with a mean ratio of 0.06 [95% confidence interval (CI), 0.02; 0.09;  $p = 0.01$ ]. A signal from  $[^{13}\text{C}]\text{bicarbonate}$  was also observed in the low-dose group after the infusion of GIK. However, the  $[^{13}\text{C}]\text{bicarbonate}/[1-^{13}\text{C}]\text{pyruvate}$  signal ratio was insignificantly greater than zero at this dose, with a mean ratio of 0.02 (95% CI,  $-0.01$ ; 0.04;  $p = 0.12$ ). A three-fold higher  $[^{13}\text{C}]\text{bicarbonate}/[1-^{13}\text{C}]\text{pyruvate}$  ratio was observed in the high-dose group compared with the low-dose group. A difference of  $-0.04$  (95% CI,  $-0.08$ ;  $-0.01$ ;  $p = 0.03$ ) between the high- and low-dose groups was observed. Post-GIK, the  $[^{13}\text{C}]\text{bicarbonate}$  signal decreased almost back to baseline level (80% decrease) ( $p = 0.005$ ) in the high-dose group. In the low-dose group, no  $[^{13}\text{C}]\text{bicarbonate}$  signal could be detected post-GIK. The effect of GIK on  $[1-^{13}\text{C}]\text{alanine}$  and  $[1-^{13}\text{C}]\text{lactate}$  was also evaluated (Fig. 2). No significant effect of GIK was observed in the low-dose group (alanine,  $p = 0.68$ ; lactate,  $p = 0.18$ ) or in the high-dose group (alanine,  $p = 0.48$ ; lactate,  $p = 0.43$ ).

### Blood glucose

Blood glucose was measured before each of the three injections of hyperpolarized  $[1-^{13}\text{C}]\text{pyruvate}$  (Fig. 3). In the fasted state, the blood glucose level was relatively low in both groups (low-dose group,  $6.7 \pm 1.6 \text{ mmol/L}$ ; high-dose group,  $5.5 \pm 0.9 \text{ mmol/L}$ ). One hour of GIK infusion resulted in an increase in blood glucose (low-dose group,  $14.9 \pm 2.5 \text{ mmol/L}$ ; high-dose group,  $17.0 \pm 5.6 \text{ mmol/L}$ ). One hour post-GIK infusion, the glucose level decreased again in both groups (low-dose group,  $8.2 \pm 1.4 \text{ mmol/L}$ ; high-dose group,  $8.5 \pm 3.8 \text{ mmol/L}$ ). An overall

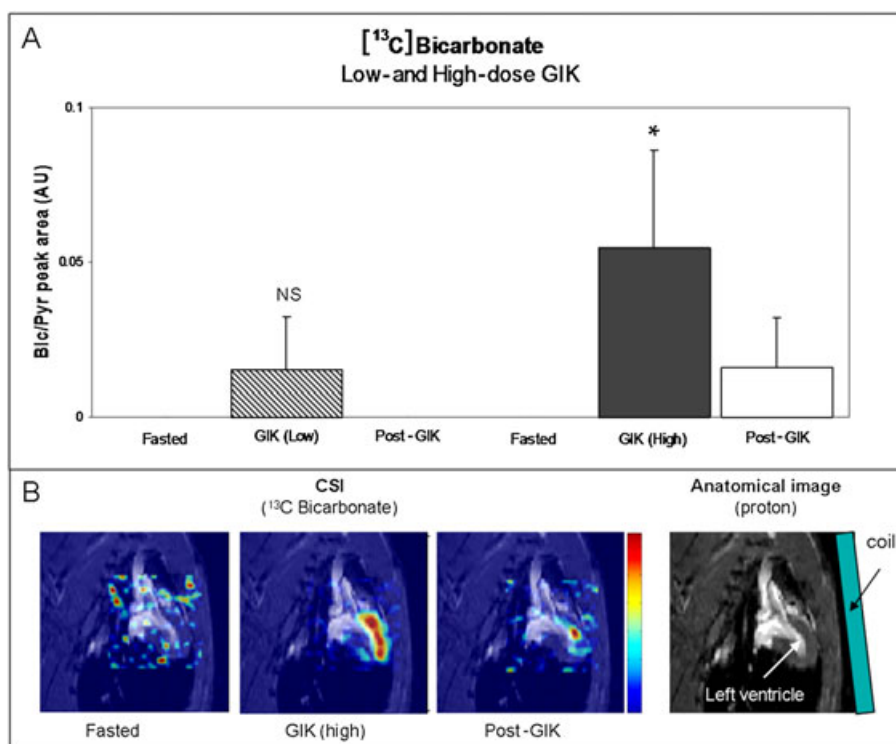


**Figure 1.** (A) Myocardial  $[^{13}\text{C}]\text{bicarbonate}/[1-^{13}\text{C}]\text{pyruvate}$  (Bic/Pyr) signal ratio in rats given high-dose and low-dose glucose, insulin and potassium (GIK) in the fasted state, after 1 h of GIK infusion and 1 h post-GIK infusion ( $*p = 0.01$  versus zero (fasted); NS, not significant). (B) Single example of chemical shift imaging (CSI) of myocardial  $[^{13}\text{C}]\text{bicarbonate}$  in the fasted state, after 1 h of GIK infusion and 1 h post-GIK infusion (high dose), and the corresponding anatomical proton image of the heart, demonstrating the position of the receive array coil.

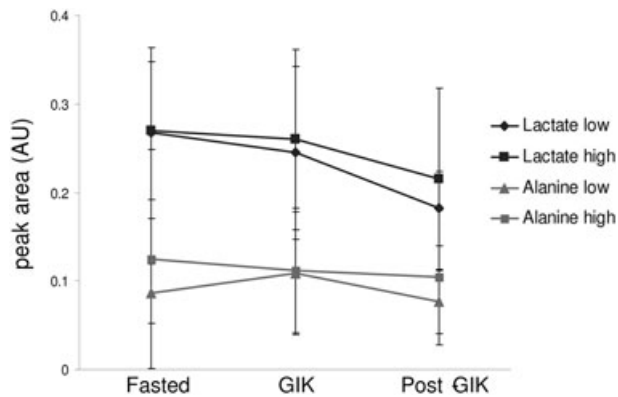


**Figure 2.**  $[1-^{13}\text{C}]$ Lactate ( $[1-^{13}\text{C}]$ lactate/ $[1-^{13}\text{C}]$ pyruvate ratio) and  $[1-^{13}\text{C}]$ alanine ( $[1-^{13}\text{C}]$ alanine/ $[1-^{13}\text{C}]$ pyruvate ratio) signals in rats given high-dose and low-dose glucose, insulin and potassium (GIK) in the fasted state, after 1 h of GIK infusion and 1 h post-GIK infusion. No significant difference in  $[1-^{13}\text{C}]$ lactate or  $[1-^{13}\text{C}]$ alanine signal could be observed after GIK infusion in either the low-dose or high-dose group.

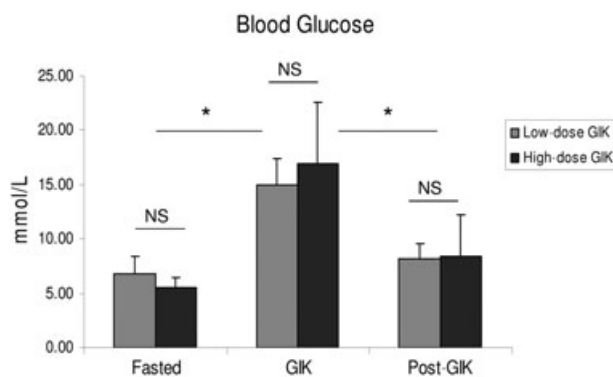


**Figure 3.** Blood glucose levels in rats given low-dose and high-dose glucose, insulin and potassium (GIK) in the fasted state, after 1 h of GIK infusion and 1 h post-GIK infusion. A significant increase was observed in the low-dose and high-dose groups ( $*p < 0.001$ ) after GIK infusion compared with the fasted state, but no significant difference was observed between the two groups (NS).

ANOVA of equal means revealed no significant difference between the high- and low-dose GIK groups ( $p = 0.197$ ). However, significant internal differences were observed between the fasted and the GIK state, as well as between the GIK and post-GIK state, in both groups (low dose: fasted versus GIK and GIK versus post-GIK,  $p < 0.001$ ; high dose: fasted versus GIK,  $p < 0.001$ ; GIK versus post-GIK,  $p = 0.002$ ).

## DISCUSSION

Two different doses of GIK were evaluated in this study. Our results suggest that a high dose of GIK is required to achieve a significantly high  $[^{13}\text{C}]$ bicarbonate signal in fasted rats. However, in fed rats, a lower concentration of plasma FA and a smaller initial inhibition of PDH activity are expected, which may increase the metabolic response to GIK. Blood glucose was found to increase to the same level independent of the infused GIK dose. This is not surprising, as the insulin dose is the same relative to glucose in the high-dose mixture as in the low-dose mixture, and the

blood glucose clearance rate (uptake of glucose from the blood into the cells) is dependent on the insulin dose.

The large variation in the  $[^{13}\text{C}]$ bicarbonate signal in both the low-dose and high-dose groups may indicate a variable PDH enzyme activity between the animals. Like other enzymes, PDH has a maximum flux limitation. It is likely that more than 1 h of infusion of GIK is required to reach the maximum PDH flux or, at least, a steady state in fasted rats, which may reduce the variation in the  $[^{13}\text{C}]$ bicarbonate signal between animals. The fast inactivation of PDH (decrease in  $[^{13}\text{C}]$ bicarbonate signal) post-GIK infusion suggests that the regulation of PDH occurs on a faster time scale than 1 h, and that a constant infusion is required to ensure high PDH flux during the hyperpolarized  $^{13}\text{C}$  MRS measurements. We cannot exclude the possibility that the variation is also caused by technical factors, such as differences in slice and/or coil positions. The CSI image (Fig. 1B) does not contain any contaminating signals from surrounding tissue, which implies that the signal from the surrounding tissue is below the detection level, and that the signal obtained from the long-axis slice originates from the heart.

Subsequent injections of pyruvate could potentially affect metabolism. However, a recent hyperpolarized  $^{13}\text{C}$  MRS study using the same pyruvate dose (1.0 mL at 80 mM) has shown that the circulating pyruvate concentration returns to baseline levels within 30 min after injection, which suggests a rapid uptake and metabolic conversion of pyruvate in various organs and blood (10).

The PDK inhibitor dichloroacetic acid (DCA) has been used recently to regulate the PDH flux in cardiac hyperpolarized  $^{13}\text{C}$  MRS studies (4,10,27). The administration of 150 mg/kg DCA was able to enhance the  $[^{13}\text{C}]$ bicarbonate signal 3.3-fold in normal fed rats (27). Although DCA has been used in metabolic research for many years, severe side-effects have been reported using much lower doses of DCA in both animals and humans (28,29). A direct comparison of the two methods of activation of PDH would be interesting. However, the administration of GIK is considered to be a more physiological and less disruptive way to enhance the  $[^{13}\text{C}]$ bicarbonate signal. Furthermore, it should be more suitable for clinical applications, as GIK infusion has already been evaluated in cardiac PET imaging in humans, and has been studied extensively in patients with acute myocardial ischaemia.

The heart's ability to shift between substrates for energy production is critical. In ischaemic heart disease and heart failure, a metabolic shift towards glucose relative to FA has been shown to represent an adaptation to a lower oxygen environment in poorly perfused areas of the myocardium, as less oxygen is required for glucose oxidation per unit ATP produced relative to FA oxidation (7). GIK infusions could potentially be used in future hyperpolarized  $^{13}\text{C}$  MRS studies to evaluate the heart's ability to shift its energy metabolism, e.g. in heart failure, diabetes or other metabolic diseases.

In conclusion, this study demonstrates that the infusion of GIK can increase significantly the signal from  $[^{13}\text{C}]$ bicarbonate in cardiac hyperpolarized  $^{13}\text{C}$  MRS measurements in fasted rats. The elevated  $[^{13}\text{C}]$ bicarbonate signal indicates an increased flux of  $[1-^{13}\text{C}]$ pyruvate through the PDH enzyme complex, and an increase in the myocardial glucose oxidation through the citric acid cycle. The regulation of myocardial metabolism by GIK infusion can potentially improve the assessment of cardiac metabolism by hyperpolarized  $^{13}\text{C}$  MRS for the evaluation of heart diseases in preclinical, as well as clinical, applications.

## Acknowledgements

The authors would like to thank Sascha Gude for her skilful technical assistance. This study was supported by grants from The Simon Spies Foundation, The Lundbeck Foundation, The Danish Heart Association and Copenhagen University Hospital Hvidovre.

## REFERENCES

- Bing RJ, Siegel A, Vitale A, Balboni F, Sparks E, Taeschler M, Klapper M, Edwards S. Metabolic studies on the human heart in vivo. I. Studies on carbohydrate metabolism of the human heart. *Am. J. Med.* 1953; 15(3): 284–296.
- Bing RJ, Siegel A, Ungar I, Gilbert M. Metabolism of the human heart. II. Studies on fat, ketone and amino acid metabolism. *Am. J. Med.* 1954; 16(4): 504–515.
- Neely JR, Morgan HE. Relationship between carbohydrate and lipid metabolism and the energy balance of heart muscle. *Annu. Rev. Physiol.* 1974; 36: 413–459.
- Atherton HJ, Dodd MS, Heather LC, Schroeder MA, Griffin JL, Radda GK, Clarke K, Tyler DJ. Role of pyruvate dehydrogenase inhibition in the development of hypertrophy in the hyperthyroid rat heart: a combined magnetic resonance imaging and hyperpolarized magnetic resonance spectroscopy study. *Circulation*, 2011; 123(22): 2552–2561.
- Kerbey AL, Randle PJ, Cooper RH, Whitehouse S, Pask HT, Denton RM. Regulation of pyruvate dehydrogenase in rat heart. Mechanism of regulation of proportions of dephosphorylated and phosphorylated enzyme by oxidation of fatty acids and ketone bodies and of effects of diabetes: role of coenzyme A, acetyl-coenzyme A and reduced and oxidized nicotinamide-adenine dinucleotide. *Biochem. J.* 1976; 154(2): 327–348.
- Orfali KA, Fryer LG, Holness MJ, Sugden MC. Interactive effects of insulin and triiodothyronine on pyruvate dehydrogenase kinase activity in cardiac myocytes. *J. Mol. Cell. Cardiol.* 1995; 27(3): 901–908.
- Stanley WC, Recchia FA, Lopaschuk GD. Myocardial substrate metabolism in the normal and failing heart. *Physiol. Rev.* 2005; 85(3): 1093–1129.
- Golman K, Petersson JS, Magnusson P, Johansson E, Akeson P, Chai CM, Hansson G, Mansson S. Cardiac metabolism measured noninvasively by hyperpolarized <sup>13</sup>C MRI. *Magn. Reson. Med.* 2008; 59(5): 1005–1013.
- Schroeder MA, Cochlin LE, Heather LC, Clarke K, Radda GK, Tyler DJ. In vivo assessment of pyruvate dehydrogenase flux in the heart using hyperpolarized carbon-13 magnetic resonance. *Proc. Natl. Acad. Sci. USA*, 2008; 105(33): 12 051–12 056.
- Atherton HJ, Schroeder MA, Dodd MS, Heather LC, Carter EE, Cochlin LE, Nagel S, Sibson NR, Radda GK, Clarke K, Tyler DJ. Validation of the in vivo assessment of pyruvate dehydrogenase activity using hyperpolarised <sup>13</sup>C MRS. *NMR Biomed.* 2011; 24(2): 201–208.
- Merritt ME, Harrison C, Storey C, Jeffrey FM, Sherry AD, Malloy CR. Hyperpolarized <sup>13</sup>C allows a direct measure of flux through a single enzyme-catalyzed step by NMR. *Proc. Natl. Acad. Sci. USA*, 2007; 104(50): 19 773–19 777.
- Schroeder MA, Atherton HJ, Ball DR, Cole MA, Heather LC, Griffin JL, Clarke K, Radda GK, Tyler DJ. Real-time assessment of Krebs cycle metabolism using hyperpolarized <sup>13</sup>C magnetic resonance spectroscopy. *FASEB J.* 2009; 23(8): 2529–2538.
- Cooper RH, Randle PJ, Denton RM. Regulation of heart muscle pyruvate dehydrogenase kinase. *Biochem. J.* 1974; 143(3): 625–641.
- Patel MS, Korotchkina LG. Regulation of the pyruvate dehydrogenase complex. *Biochem. Soc. Trans.* 2006; 34(Pt 2): 217–222.
- Muniyappa R, Montagnani M, Koh KK, Quon MJ. Cardiovascular actions of insulin. *Endocr. Rev.* 2007; 28(5): 463–491.
- Kurien VA, Oliver MF. Serum-free-fatty-acids after acute myocardial infarction and cerebral vascular occlusion. *Lancet* 1966; 2(7455): 122–127.
- Oliver MF, Kurien VA, Greenwood TW. Relation between serum-free-fatty acids and arrhythmias and death after acute myocardial infarction. *Lancet* 1968; 1(7545): 710–714.
- Opie LH. Metabolism of free fatty acids, glucose and catecholamines in acute myocardial infarction. Relation to myocardial ischemia and infarct size. *Am. J. Cardiol.* 1975; 36(7): 938–953.
- Schipke JD, Friebe R, Gams E. Forty years of glucose–insulin–potassium (GIK) in cardiac surgery: a review of randomized, controlled trials. *Eur. J. Cardiothorac. Surg.* 2006; 29(4): 479–485.
- Bax JJ, Visser FC, Poldermans D, Van LA, Elhendy A, Boersma E, Visser CA. Feasibility, safety and image quality of cardiac FDG studies during hyperinsulinaemic–euglycaemic clamping. *Eur. J. Nucl. Med. Mol. Imaging* 2002; 29(4): 452–457.
- Knuuti MJ, Nuutila P, Ruotsalainen U, Saraste M, Harkonen R, Ahonen A, Teras M, Haaparanta M, Wegelius U, Haapanen A. Euglycemic hyperinsulinemic clamp and oral glucose load in stimulating myocardial glucose utilization during positron emission tomography. *J. Nucl. Med.* 1992; 33(7): 1255–1262.
- Gropler RJ, Siegel BA, Lee KJ, Moerlein SM, Perry DJ, Bergmann SR, Geltman EM. Nonuniformity in myocardial accumulation of fluorine-18-fluorodeoxyglucose in normal fasted humans. *J. Nucl. Med.* 1990; 31(11): 1749–1756.
- Martin WH, Jones RC, Delbeke D, Sandler MP. A simplified intravenous glucose loading protocol for fluorine-18 fluorodeoxyglucose cardiac single-photon emission tomography. *Eur. J. Nucl. Med.* 1997; 24(10): 1291–1297.
- Moreno KX, Sabelhaus SM, Merritt ME, Sherry AD, Malloy CR. Competition of pyruvate with physiological substrates for oxidation by the heart: implications for studies with hyperpolarized [1-<sup>13</sup>C]pyruvate. *Am. J. Physiol. Heart Circ. Physiol.* 2010; 298(5): H1556–H1564.
- Ardenkjaer-Larsen JH, Fridlund B, Gram A, Hansson G, Hansson L, Lerche MH, Servin R, Thaning M, Golman K. Increase in signal-to-noise ratio of > 10,000 times in liquid-state NMR. *Proc. Natl. Acad. Sci. USA*, 2003; 100(18): 10 158–10 163.
- Vanhuffel S. Enhanced resolution based on minimum-variance estimation and exponential data modeling. *Signal Process.*, 1993; 33(3): 333–355.
- Mayer D, Yen YF, Josan S, Park JM, Pfefferbaum A, Hurd RE, Spielman DM. Application of hyperpolarized [1-(13)C]lactate for the in vivo investigation of cardiac metabolism. *NMR Biomed.* 2012; 25(10): 1119–1124.
- Stacpoole PW, Henderson GN, Yan Z, Cornett R, James MO. Pharmacokinetics, metabolism and toxicology of dichloroacetate. *Drug Metab. Rev.* 1998; 30(3): 499–539.
- Stacpoole PW. The dichloroacetate dilemma: environmental hazard versus therapeutic goldmine—both or neither? *Environ. Health Perspect.* 2011; 119(2): 155–158.



